Department of Engineering and Safety

Simplified Representation of Degradation, Inspection and Maintenance in a Strategic Decision Support Tool for Offshore Wind Operation and Maintenance

Azeem Hussain

Master thesis in Technology and Safety, August 2016

Simplified Representation of Degradation, Inspection and Maintenance in a Strategic Decision Support Tool for Offshore Wind Operation and Maintenance

Master thesis in Technology and Safety

Author: Azeem Hussain

Supervisors:
Maneesh Singh — UiT The Arctic University of Norway
Thomas Michael Welte — SINTEF ENERGY RESEARCH
Iver Bakken Sperstad — SINTEF ENERGY RESEARCH

August, 2016

UiT / THE ARCTIC UNIVERSITY OF NORWAY

Summary:

The global demand for energy is increasing in the current scenario of industrial development and offshore wind energy has a great potential to become a key player specifically in Europe's renewable energy future. Naturally the flow of wind in offshore environments is more consistent and also the average wind velocity is higher than onshore. However, the cost of electricity generated from offshore wind turbines is higher currently and the challenge of cost reduction is at the top priority. Operation and maintenance costs are the main contributor to the life cycle cost of the offshore wind energy farms. A great proportion of operation and maintenance costs has been assigned to corrective replacement of major components of the wind turbines. Mathematical optimization models are frequently used in the maintenance management to lower the cost of maintenance and failure. To overcome the overhead expenses, the strategic decision support tools for offshore wind operation and maintenance such as NOWIcob (Norwegian Offshore Wind cost benefit model) can be used to investigate strategies for major components. In the current situation, the NOWIcob model is not able to capture the degradation of components with time and also how the degradation can be detected by inspections or condition monitoring systems. To implement degradation and inspection in NOWIcob, a simple/loose integration technique has been employed by developing the so called translators from detailed degradation models to be used as input into the NOWIcob. For this purpose, the linear elastic fractures mechanics model based on Paris Law and Gamma process has been used for degradation modelling approach. Monte Carlo simulations were applied to simulate the degradation paths and subsequently obtain the failure time and prewarning time.

Acknowledgements

With the accomplishment of my Master's thesis at the Department of Engineering and Safety UiT The Arctic University of Norway, a magnificent phase of my life as a student in Tromsø has completed. During this I have learned a lot about safety engineering and technology from the best people. I would like to thank my supervisor Professor Maneesh Singh for being supportive and thought provoking during studies, and his continuous motivation makes me move forward. Also I would like to thank specially our course coordinator Jawad Barabady for provinng me this opportunity of great learning and all the support during the degree.

The time I have spent at SINTEF ENERGY RESEARCH during my thesis work have been a remarkable experience of learning about offshore wind operation and maintenance. In this regard, I would like to thank Thomas Michael Welte and Iver Bakken Sperstad for their valuable time and guidance during my stay in Trondheim. Also specially, Thomas for being always available to help and explain from the start of the project till the compilation of the thesis has completed with detailed comments and discussions.

I would lile to thank all my colleagues within the Department of Engineering and Safety for their positive discussions and a nice environment during my stay. In particular, I sincerely appreciate all the time and positive suggestions by Azeem Ahmad during this project. Your great company will always be remembered.

Last but not the least, I would like to thank Zeeshan, Najeeb, Faisal, Intisab, Tanvir, my fellow valuable friends in Tromsø, my family for supporting me during this project. You all people provided the required assisstance in your own way, I greatly appreciate this.

Tromsø, August 2016
Azeem Hussain

Table of Contents

Chapter 1

Introduction

1.1 Research Context

The global energy demand is rising, this is mainly because of growing population and economic development. During the previous 20 years the worldwide population has increased by 1.6 billion people. Though the growth rate is trending down, the population is presumed to raise 1.4 billion over the next 20 years. Also the global gross domestic product (GDP) growth is expected to accelerate, pushed by low and medium income economies.

The energy efficiency, which is expressed as energy over GDP, will continue to increase worldwide. Despite these expansions in energy efficiency, a total surge of global energy demand of 80% is anticipated by 2035. Moreover, the fuel mix variates slowly as gas and non-fossil fuels achieve share at the cost of coal and oil. The swiftest emerging fuels are renewables, International Energy Agency, 2016 (Figure 1).

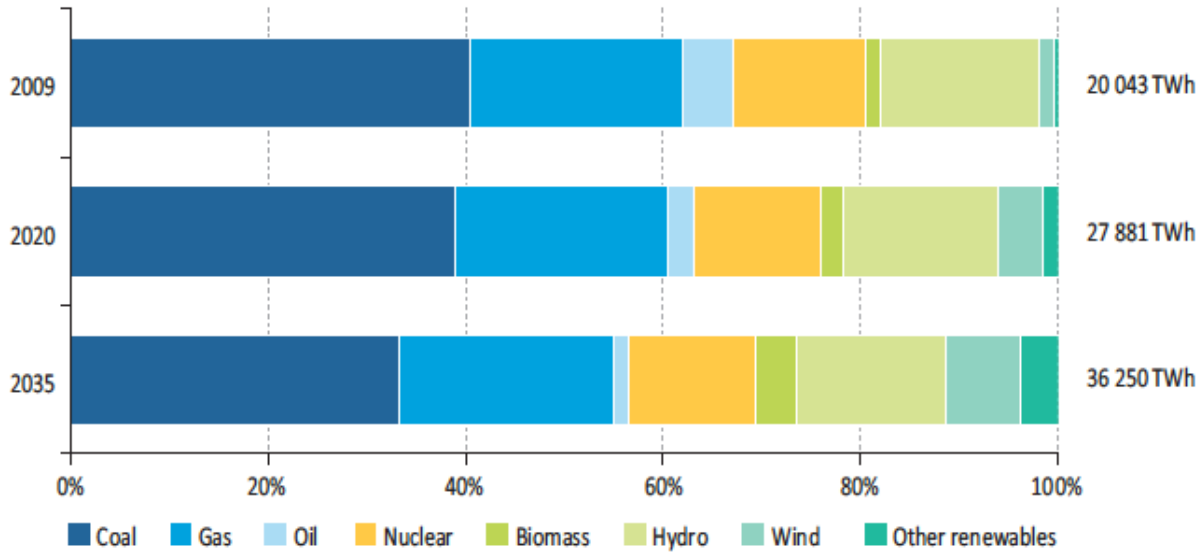

Figure 1 Share of world electricity generation (International Energy Agency, 2016)

1.2 Wind Energy

Wind energy is kinetic energy of wind used for electricity generation in wind turbines. Wind energy, like other power technologies based on renewable resources, is widely available throughout the world and can contribute to reduced energy import dependence. Offshore wind energy indicates to the energy generated by wind turbine installed in the sea. Subjected to the depth of the sea, the installation area can be several tens of kilometers off the shoreline.

Installing turbines in the sea takes advantage of better wind resources than at land-based sites. Offshore turbines, hence, attain considerably more full-load hours. Extensive offshore deployment has commenced mostly in Europe. In 2014, global offshore wind generated an anticipated 25 TWH, 20% higher than in 2013 and worldwide installed capacity of offshore wind touched over 8.8 GW, with 1.7 GW of new additions versus 2012 (International Energy Agency, 2016).

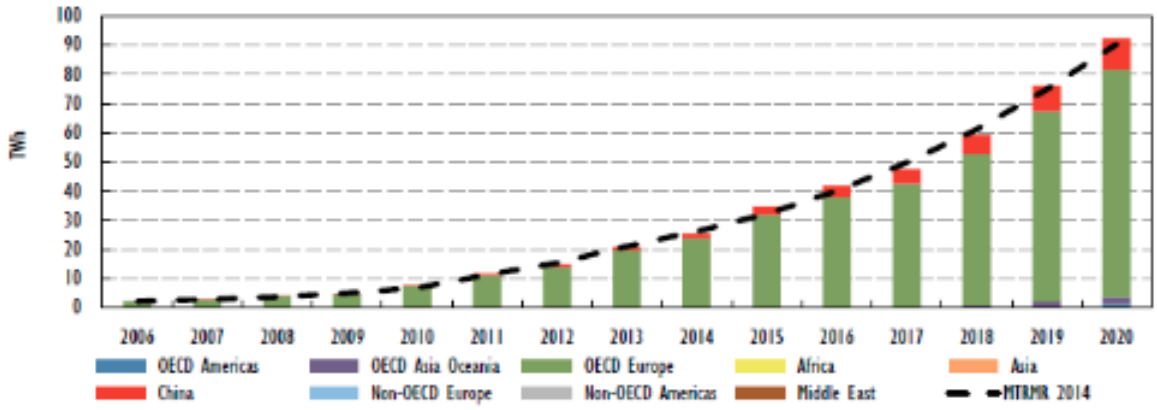

Figure 2 Offshore wind generation forecast and projection (International Energy Agency, 2016).

1.3 Offshore Wind Turbine

An offshore wind turbine (OWT) comprises of many components (Figure 3). The most important one are discussed below

The **nacelle** includes the generator, the gearbox and all other modules to transform wind energy into electrical energy.

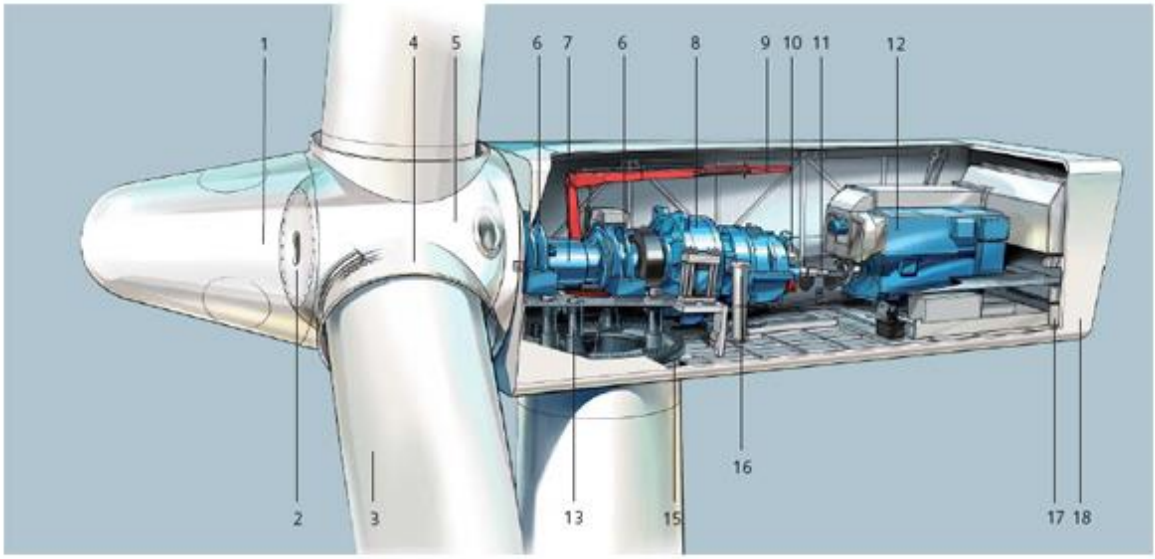

Nacelle Arrangement

1 Spinner	**10** Brake disc
2 Spinner bracket	**11** Coupling
3 Blade	**12** Generator
4 Pitch bearing	**13** Yaw gear
5 Rotor hub	**14** Tower
6 Main bearing	**15** Yaw ring
7 Main shaft	**16** Oil filter
8 Gearbox	**17** Generator fan
9 Service crane	**18** Canopy

Figure 3 Wind Turbine SWT-3.6-120 (Siemens Wind Power)

The **rotor** contains the hub and the blades. The blades are attached to the hub, which transfers the rotational energy to the gearbox via the main shaft. The extent of blades can be up to 75 meters in length.

The **tower** delivers support to the rotor-nacelle-assembly (RNA) and consists of a tubular structure and is assembled of several sections. The characteristic tower height ranges between 80-130 meters.

The **transition piece** unites the tower to the foundation pile. Next to this, a boat landing, an access deck and ladder can be mounted on the transition piece which provides entrance to the tower. This component might not be present always.

The **foundation** provides support to the wind turbine in offshore environments. Various types of foundation structures exist (Figure 4) and are deployed on the basis of water depth.
The tower, transition piece and foundation collectively called as the support structure and the rotor-nacelle-assembly (RNA) consists of the rotor and the nacelle.

1.3.1 Steel Structure Concepts

According to the DNV GL (2016), the typical steel support structures can be of following type,

1.3.1.1 Tubular Towers

A common tower design for both onshore and offshore wind turbines are tubular steel towers, which are manufactured in tubular sections typically of 20-30 m length with flanges at both ends. The tower will typically have circular cross-sections.

1.3.1.2 Segmented Towers

The cross-sections in the segmented steel tower are divided into a number of steel panels which typically are assembled by bolts. A key advantage for a segmented tower design is the facilitation of transportation.

1.3.1.3 Lattice Towers

Lattice towers are typically manufactured by means of welded or bolted tubular steel profiles or L-section steel profiles. The lattice towers are typically three-four-legged and consist of corner chords interconnected with bracings in a triangulated structure.

1.3.2 Offshore Monopile Substructures/Foundations

The monopile structure is a simple design by which the tower is supported by one large pile, either directly or through a transition piece, which is a transitional section between the tower and the monopile. The monopile continues down into the seabed to a depth where it is fully anchored. The monopile structure is typically made of circular steel tubes and fabricated in one piece. If a transition piece is used this is typically equipped with accessories and is installed on the monopile after the pile has been fixed. Transition piece is made up of circular steel tubes and is fabricated as one piece.

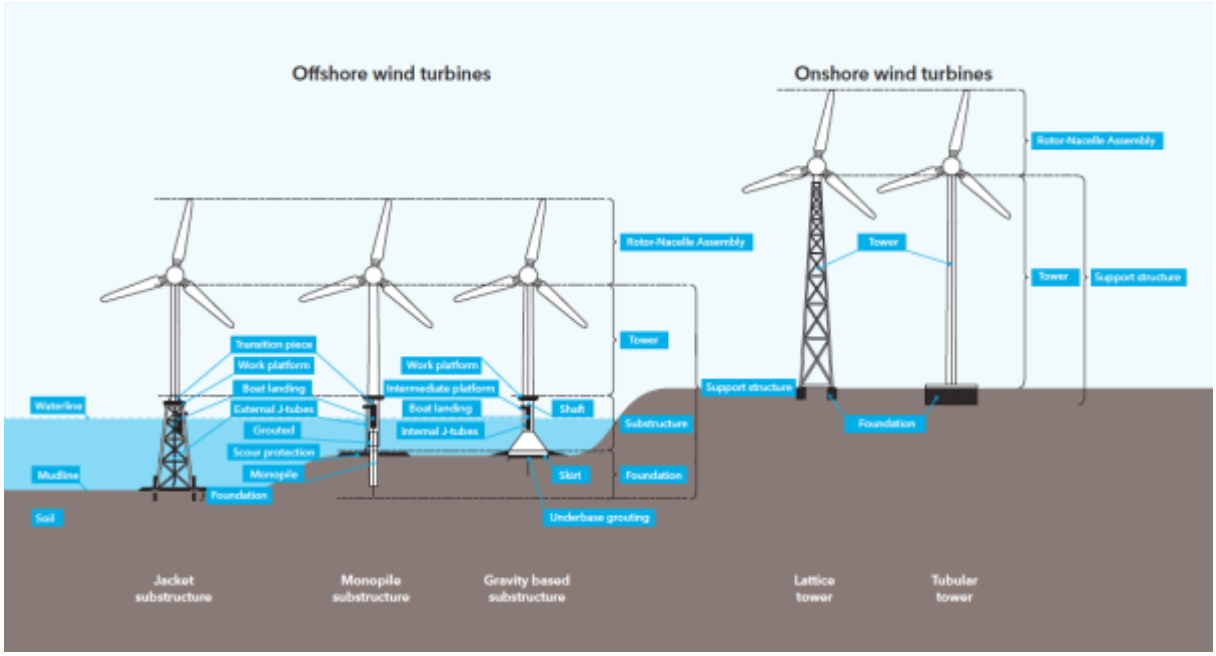

Figure 4 Various types of offshore wind turbine support structures, from left to right jacket, monopile, gravity, tripod, and gravity based foundations DNVGL, 2016.

1.3.3 Offshore Jacket Substructures/Foundations

Jacket substructures/foundations are classically three-or four-legged triangulated structures all made of circular steel tubes. On top of the jacket structure is installed a transition piece, typically a plated structure, which is designed with a large center steel tube for connection with the tower. The jacket is typically anchored into the seabed by piles installed at each jacket leg.

1.3.4 Offshore Tripod Substructures/Foundations

The tripod substructure/foundation is a standard three-legged structure made of circular steel tubes. The central steel shaft of the tripod makes the transition to the wind turbine tower. The tripod can have either vertical or inclined pile sleeves.

1.3.5 Offshore Jacket and Tripods with Suction Buckets

The jacket/tripod substructures/foundations with suctions buckets are structures equipped with suction bucket foundations at each leg instead of piles as for the conventional jacket/tripod structure. The use of the suction buckets eliminates the need for driving of piles as required for the conventional jacket/tripod substructures/foundations.

1.3.6 Offshore Suction Mono-bucket Foundations

The suction mono-bucket steel structure usually comprises of a center column attached to a single large steel bucket through flange-reinforced shear panels, which distribute the loads from the center column to the edge of a large bucket. The wind turbine tower is joined to the substructure center column above mean sea level. The bucket is fixed by means of suction and will in the permanent case behave as a gravity-based foundation, relying on the weight of the soil encompassed by the steel bucket with a skirt length of approximately the same dimension as the width of the bucket.

1.4 Background of the Research Project

Operation and maintenance (O&M) costs enhance significantly to the cost of energy of offshore wind farms, and a large percentage of the O&M cots can be ascribed to corrective replacement of major components such as gear boxes or main bearings. Not only does the replacement of such components require specialist (jack-up) vessels with very high day rates, but the downtime coupled with the replacement is also large, since the lead time for chartering such vessels usually is of the order of months. Strategic decision support tools for offshore wind O&M, such as the NOWIcob (Norwegian Offshore Wind cost benefit model) developed by SINTEF ENERGY RESEARCH, can be used to investigate strategies for major components and other aspects of the overall O&M strategy for the wind farm. This master's thesis is related to the ongoing research in the LEANWIND (Logistic Efficiencies And Naval architecture for Wind Installations with Novel Development) project, which is a EU project led by 31-partner consortium. SINTEF Energy's role in this project is the development of simulation model to study maintenance strategies and cost benefit assessment technologies developed in the rest of the project. The main objective of this project is to introduce so-called 'lean' principles to offshore wind industry to reduce the energy costs from the wind energy(SINTEF Energy Research, 2016).

In order to lower the cost of maintenance and failure, mathematical optimization models are progressively applied in the field of maintenance management. A distinctive feature of optimizing maintenance is that decisions often must be made under uncertainty (such as in deterioration and cost). In maintenance management, the most important uncertainty is generally the uncertainty in the time to failure (lifetime) and/or the rate of deterioration.

1.5 Research Question:

Currently the NOWIcob model is not able to explicitly capture the degradation of components over time and how degradation maybe detected by inspections or condition monitoring systems. (Hofmann, Sperstad and Kolstad, 2015). For real wind farms, decision rules based on information about the degradation of a component could be a part of the maintenance strategy for the degrading component. One question, however, is how important it is for the assessment of a wind farm O&M strategy to include such detailed degradation models in NOWIcob, or whether a simple, high-level representation would be sufficiently accurate. This means that there are two alternatives for implementing/representing degradation in NOWIcob:

1) **Full integration**, i.e. complete implementation of one or several degradation models in the NOWIcob decision support tool.
2) **Simple/loose integration,** i.e. simplified integration of degradation, inspection and maintenance in the NOWIcob decision support tool by "translating" input and output from detailed models on degradation, inspection and maintenance to input that can be used by existing NOWIcob input modules.

One goal of current research work in the LEANWIND project is to compare the different alternatives and answer the question if the simplified integration (described in 2) is sufficient for typical NOWIcob applications.

1.6 Aim of the Project:

The aim of the masters' thesis is to contribute to provide an answer to the problem and questions formulated above. The existing NOWIcob modules require a number of input parameters that are not the same as used in the degradation models. So the parameters used in the detailed models must be "translated" into the required input for NOWIcob. The aim of the master's thesis is to suggest and develop so-called "translators" for selected type of degradation models and testing of the translators in NOWIcob. There are several modules that can be used for providing input to NOWIcob (e.g, module for corrective maintenance and preventive maintenance tasks), so there could be several choices for the loose integration of the detailed degradation/inspection/ maintenance models and in this regard different

translators could be developed for the same type of model. The comparison and assessment of the translators for the different alternatives is the part of the master thesis work.

There are many possibilities for developing the translators. Analytical methods could be practicable for some cases. But many problems cannot be resolved analytically. So, numerical methods and simulations (e.g., Monte Carlo simulations) should be used. To become familiar with such models and develop program code for execution of numerical analysis and simulations is part of the master thesis work. The methods that will be used and the results will be described and discussed in the thesis.

1.7 Outline of the Project:

The following chapters are written in this sequence. Chapter 2 describes about the loads on an offshore wind turbine and structural integrity. Chapter 3 gives an introduction to degradation models and chapter 4, a brief description of NOWIcob model. Chapter 5 explains about the methods employed during the analysis. Chapter 6 explains the modeling approach, which has been employed during the master's thesis project. This chapter is the link between previous chapters, i.e., how the degradation modeling approach will be linked to the NOWIcob model to explicitly capture the degradation of components over time and how the degradation can be detected by inspections and condition monitoring systems. The last chapter 7 discusses about the conclusions and recommendations for further work.

Chapter 2

Loads on an Offshore Wind Turbine and Structural Integrity

Loading on Structures

2.1 Design Loads for Offshore Wind Turbine Structures

According to Malhotra, 2009, an offshore wind turbine is exposed to three forms of loads during operation, loads due to waves, wind and operational loads. Wind loading is the principal loading on an offshore wind turbine structure, it effects the dynamic characteristics that are unlike from the wave and current loading that governs the design of foundations for classic oil and gas installations. The loading on wind turbine foundations is described by comparatively small vertical loading and big horizontal and moment loads which are also dynamic. The design loads are categorized into permanent, variable and environmental loads.

2.2 Permanent Loads

Permanente loads are the loads that will not fluctuate in magnitude, position or direction during the period considered. These loads comprise of mass of the structure in air, pre-tension loads, the mass of grout and ballast, equipment, or accessories which are permanently attached to the access platform and hydrostatic forces on the several members underneath the waterline. These forces involve buoyancy too. The characteristic value of a permanent load is defined as the expected value based on accurate data of the unit, mass of the material and the volume in question

2.3 Variable Loads

Variable loads are the loads that can fluctuate in magnitude, position and direction throughout the consideration period. These loads can come from personnel, crane operations, ship collisions from service vessels, loads from fendering, entrance ladders, platforms and adjustable ballast and additionally actuation loads. Actuation loads produced from the

operation of the wind turbine, which involves torque control from the generator, yaw and pitch actuator loads and mechanical braking loads. Additionally, gravity loads on the rotor blades, centrifugal and Coriolis forces, and gyroscopic forces due to yawing are included in design. Loads that appear throughout fabrication and installation of the wind turbine or its components likewise categorize as variable loads. During fabrication, erection lifts of various structural components produce lifting forces, however in the installation stage forces are produced during load out, carrying to the site, launching and upending, as well as through lifts linked to installation. Forces produced in the operational phase are frequently dynamic or impulsive.

2.4 Environmental Loading

Environmental loads depend on the site climate and involve loads from wind, wave, ice, currents and earthquakes and have a larger amount of uncertainty related with them (Figure 5). These loads depend upon time, covering a widespread range of time episodes fluctuating from a fraction of a second to several hours. These loads act on the wind tower across distinctive load combinations and directions under dissimilar design conditions and are divided into an axial force, horizontal base shear, an overturning moment and torsional moment to be repelled by the foundation (Malhotra, 2009).

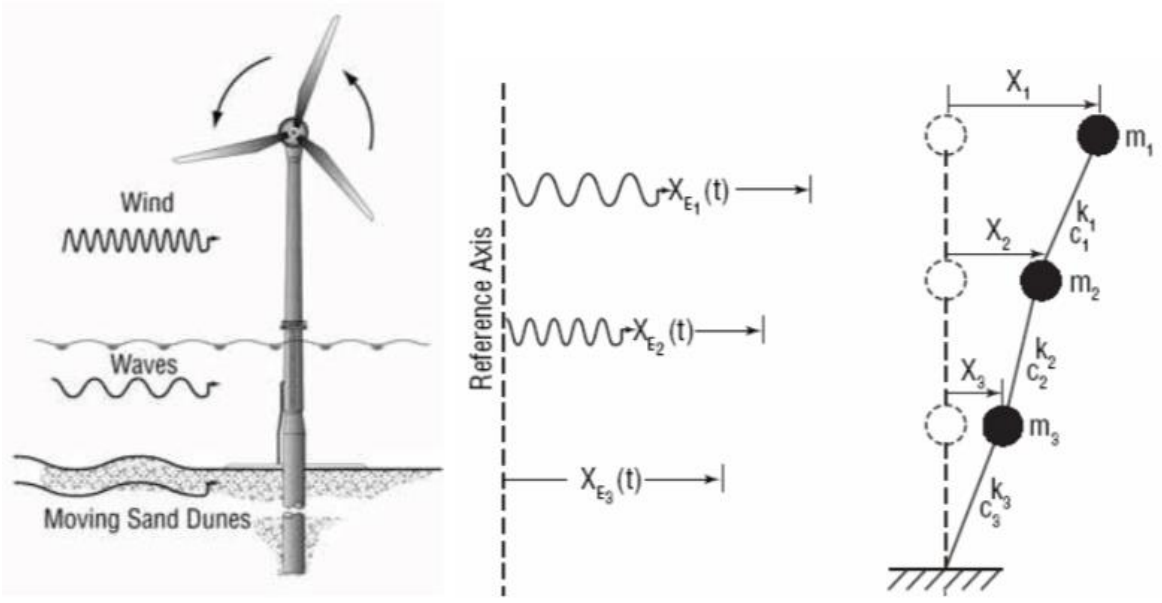

Figure 5 Loads from wind, waves, currents, and moving sand dunes(Malhotra, 2009)

2.4.1 Wind Loading

Site specific wind data collected over sufficiently long periods are usually required to develop the wind speed statistics to be used as the basis of design. The design wind is represented by a mean wind speed, a standard deviation and a probability distribution for each of these parameters. Wind speed data are height dependent. To develop a design wind speed profile, a logarithmic or an exponential wind speed profile is often used. In areas where hurricanes are known to occur the annual maximum wind speed should be based on hurricane data.

2.4.2 Hydrodynamic Loads

Site specific measured wave data collected over long continuous periods are preferable. When site specific wave data are unavailable, data from adjacent sites must be transformed to account for possible differences due to water depths and different seabed topographies. Because waves are caused by winds, the wave data and wind data should correlate. However, extreme waves may not occur in the same direction as an extreme wind. Therefore, the directionality of the waves and wind should be recorded.

2.4.3 Loads from Currents

Tidal and wind generated currents such as those caused by storm surge have to be included in the design. In shallower waters usually a significant component of the hydrodynamic load is from currents.

2.4.4 Ice Loads

In areas where ice is expected to develop or where ice may drift ice loads have to be considered in design. The relevant data for sea ice conditions include the concentration and distribution of ice, the type of ice, mechanical properties of ice, velocity and direction of drifting ice, and thickness of ice.

2.4.5 Seismic Loads

For wind turbines to be located in seismic areas, a site response spectrum is usually developed for horizontal and vertical directions. For the analyses, the wind turbine is represented by a lumped mass at the top of the tower and it includes the mass of the nacelle, the rotors and part

of the tower. Buckling analyses of the tower are conducted with the loads from the vertical ground acceleration.

2.5 Structural Integrity of an Offshore Wind Monopile Structure

The first large offshore wind farm is approaching towards its designed lifetime soon in the forthcoming years, which was estimated to be around 25 years. The extension of the operational life of this wind farm beyond its design lifetime facilitates to escalate return on investment of wind projects. To evaluate if the safe and cost-effective operation continuation is realistic, precise evaluation of remaining practical lifetime of all offshore wind turbine components is required. A critical factor for lifetime extension is structural integrity of support structures.

Offshore wind monopiles are the major support structures deployed in shallow and intermediate water depths (Figure 6). The design of monopiles is usually fatigue-driven as OWTs are exposed to long-term, variable-amplitude aerodynamic and hydrodynamic loading. Large uncertainties in environmental loading, material resistance, and design models cause the physical properties and consequently lifetimes of installed OWTs often differ from design assumptions (Ziegler et al, 2016). According to Kallehave et al. (2015) the first natural frequency of monopiles is generally under-predicted in design (up to 20%). Fatigue lifetime estimates essentially be revised with data from on-site inspections and monitoring data.

In the offshore wind industry, damage calculation with SN-curves is generally applied for fatigue design as suggested in relevant design standards (DNVGL-ST-0126). SN-curves indicate the number of cycles of stress amplitudes until material failure, usually expressed as through-thickness crack, but without any information of propagation of fatigue cracks. Fracture mechanics methodologies are appropriate for lifetime updating established on crack inspections, because they describe all three relevant fatigue stages, a) crack initiation, b) crack propagation and c) brittle failure.

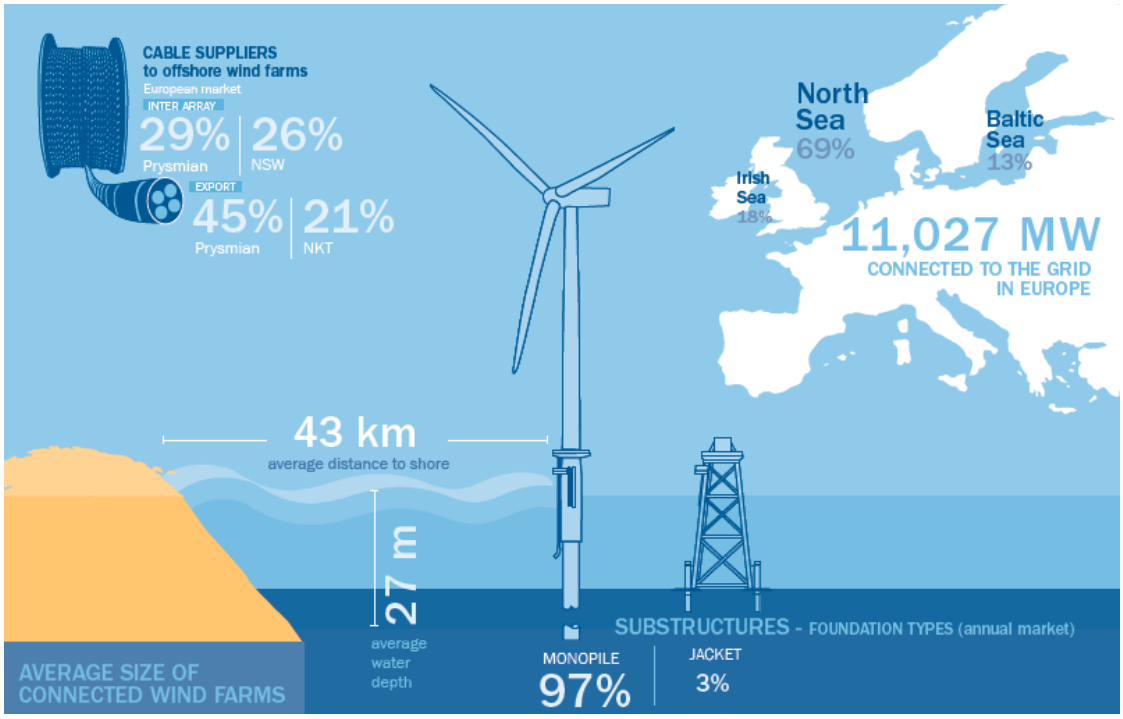

Figure 6 Offshore wind monopile and jacket substructure foundation types (International Energy Agency, 2016).

2.6 Limit states

According to DNV GL (2016), a limit state is a condition beyond which a structure or structural component will no longer fulfill the design requirements. The following three types of limit states are generally being considered at the design stage.

1) Ultimate limit states (ULS) relate to the maximum load-carrying resistance
2) Fatigue limit states (FLS) correspond to failure due to the effect of dynamic loading
3) Accidental limit states (ALS) relate to (a) maximum load-carrying capability for (exceptional) accidental loads or (b) post-accidental integrity for damaged structures.
4) Serviceability limit states (SLS) correspond to acceptance criteria related to normal use.

Following are the examples of limit states related to each category:

1) Ultimate Limit States (ULS)

- loss of structural resistance (extreme yielding and buckling)
- failure of components owing to brittle fracture
- loss of static equilibrium of the structure, or of a part of the structure, considered as a rigid body, e.g. overturning or capsizing

- failure of critical components of the structure produced by surpassing the ultimate resistance (which in some cases is reduced due to repetitive loading) or the ultimate deformation of the components
- conversion of the structure into a mechanism (collapse or extreme deformation).

2) Fatigue Limit States (FLS)

- growing damage due to repeated loads.

3) Accidental Limit States (ALS)

- structural damage produced by accidental loads (ALS type 1)
- ultimate resistance of damaged structures (ALS type 2)
- loss of structural integrity after local damage (ALS type 2).

4) Serviceability Limit States (SLS)

- deflections that might change the effect of the acting forces
- unnecessary vibrations generating discomfort or affecting non-structural components
- excessive vibrations affecting turbine operation and energy production
- deformations or motions that surpass the limitation of equipment durability
- differential settlements of foundations soils producing intolerable tilt of the wind turbine
- temperature produced deformations.

2.7 Inspections Planning for Fatigue Cracks in Offshore Structures

Degradation of offshore structures is triggered (is a consequence) of the loads (fatigue), or of chemical mechanisms (corrosion). And corrosion and wear are typical degradation/failure mechanisms. The influence of corrosion is designed for by corrosion allowance or a protection system, which makes the corrosion expansion slow and relatively easy to control. The fatigue crack growth can be more severe since cracks can result in an unexpected failure when exposed to large storm loads. Furthermore, cracks are difficult to detect because they are small for a significant part of the crack growth time (DNVGL-RP-0001).

Defects much larger than those implicit in fatigue design curves are also important to be

analyzed as observations of some cracks discovered during inspections can be attributed to such defects. Therefore, these defects are assumed to be considerably larger than those included in a probabilistic fatigue analysis. Such large defects are also sometimes denoted as gross errors. So, the following safety principles should be implemented:

- design for suitable fatigue life involving design fatigue factors (DFFs) and a comprehensive corrosion protection system
- design for robustness in relation to member failure
- plan inspection of the structure during fabrication as well as during the service life.

According to DNVGL-RP-0001, once inspections priorities are set, the potential of gross fabrication flaws should also be measured. Because inspections after fabrication onshore can be executed at less cost and with greater reliability than during operation offshore, it is valuable to emphasize these inspections, at least for components which are important for the reliability of the structures.

Diverse inspection approaches may be applicable for different types of offshore structures. This is because the prevailing structures have different strength with respect to fatigue cracking and since inspection, repair and failure costs differ considerably. A sketch to show the evaluation and development of an inspection plan for a detail is shown in Figure 7.

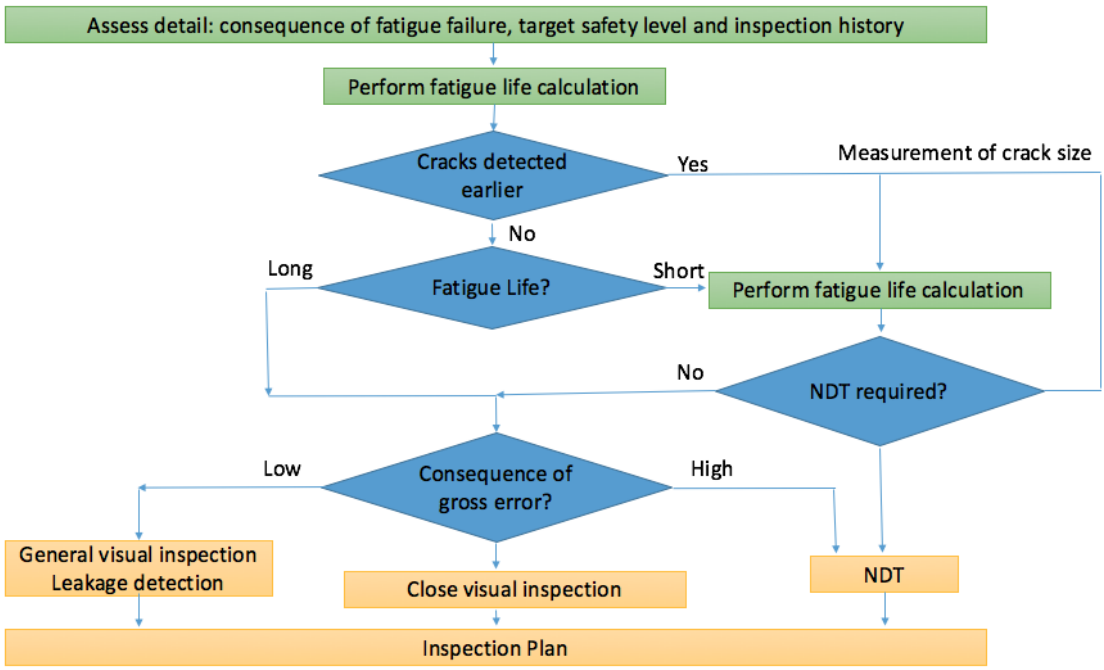

Figure 7 Schematic Development of inspection plan with respect to fatigue(DNVGL-RP-0001)

Jackets having four or more legs are redundant structures when X-type bracing is used. The effect of a fatigue crack will nevertheless be reliant on position of crack and type of loading and likelihood for redistribution of stresses during crack growth. For most hot spots there is a substantial crack growth phase before the reliability of the structure turn out to be a major concern. It might happen that cracks have been identified during earlier inspections, but have been considered to not need a repair before next inspection is executed.

2.8 Probability of Detection

Inspection Reliability for Relevant Inspection Methods

According to DNVGL (2015), non-destructive testing (NDT) is normally employed to identify and size the defects in structures. The detection ability for the NDT is stated as a function of a defect size, through probability of detection (PoD) curves. These curves are specified for the subsequent inspection methods and are presented in Figure 8 :

- flooded membrane detection (FMD)
- eddy current (EC)
- magnetic particle inspection (MPI)
- alternating current field measurement (ACFM)

General visual inspection (GVI) and close visual inspection (CVI) are considered effective for usual evaluation of the condition of the structures, but can barely be used to spot fatigue cracks before the size of the cracks has developed large in length or through the plate thickness. Complete cleaning for marine growths is critical in order to be able to find fatigue cracks.

2.8.1 Flooded Membrane Detection

FMD method is utilized for inspection of across thickness cracks in braces in jacket structures. This approach can be used for the parts that are not water filled from installation as braces (with possible fatigue crack on the brace side and not on the leg side that generally is water filled) or joints that have not been hardened by grout. The reliability of this inspection

method is considered to be good and a probability of detection equal to 0.95 can be expected.

While using FMD, it should be recognized whether throughout thickness cracks at hot spots can be accepted based on needed capacity for ultimate load. Experience indicates that FMD is competent for conductor frames in jacket structures where out-of-plane moments contribute significantly to the computed fatigue damage. Capacity for ultimate load is here of less concern than for the main load carrying braces.

2.8.2 Leakage Detection

Leakage detection can be taken as a reliable barrier with respect to fatigue crack detection in semisubmersibles and FPSOs. It is supposed that this technique can only be trusted in redundant structures where the plated structures show material with appropriate fracture toughness. When relying on leakage detection, it should be established that there is enough time from a substantial probability of detecting a fatigue crack until failure such that a repair can be executed if required.

2.9 Probability of Detection (PoD) Curves for Eddy Current, Magnetic Particle Inspection and Alternating Current Field Measurement

The distribution functions for PoD for EC, MPI and ACFM are supposed to be alike and can be written as

$$PoD(a) = 1 - \frac{1}{1 + \left(\frac{a}{X_o}\right)^b}$$

where,

a = crack depth in mm

X_o = distribution parameter (= 50% median value for the PoD)

b = distribution parameter

The probability of detection curves are dependent on qualification and execution of work. If no other documentation is provided, the PoD curves in Figure 8 can be used.

Table 1 PoD curves for EC, MPI, ACFM

Description	X_o	b
At ground welds or similar good conditions above water	0.40	1.43

Normal working conditions above water	0.45	0.90
Below water and less good working conditions above water	1.16	0.90

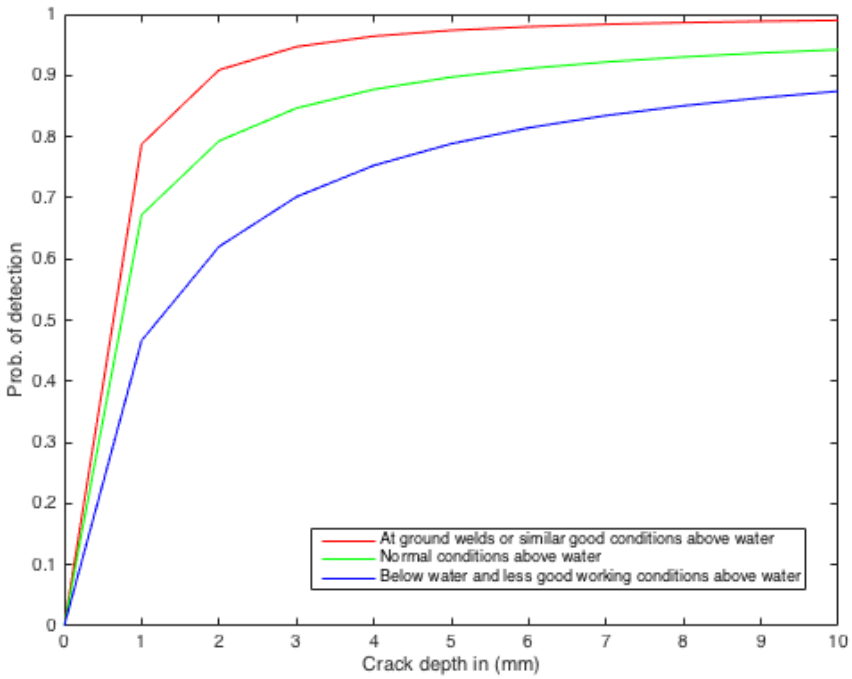

Figure 8 PoD curves for EC, MPI and ACFM (DNVGL-RP-0001)

Eddy Current is a right inspection technique throughout service life as it can be used to spot fatigue cracks without removing coating. Previously it was usual practice to perform inspection of surface cracks by Magnetic Particle Inspection, but, then the coating had to be removed. It was difficult to put back a good quality of the coating and local corrosion was spotted at the inspected areas. Now MPI is being used to validate crack clues detected by EC as this inspection method also can give false indications.

The physics in employing Eddy Current above water is only slightly different from underwater applications and, though working conditions can be stricter under water, these are balanced for by unique quality assurance methods, like using slave monitors. A parallel performance as under water is thus also probable above water, and the created PoD curve is considered expressive also for above water applications.

Alternating Current Field Measurement (ACFM) is used for identifying and sizing surface breaking flaws. ACFM has been established as an addition of the successful alternating current potential drop (ACPD) method. It was originally considered for use under water to

identify defects in offshore structures and to overcome the fact that ACPD was inappropriate for such applications because of the demand for suitable electrical contact between probes and the structure's surface. Now, however, ACFM is also employed to structures both in and out of the water. (It has the benefit over some other techniques that the structure demands slight cleaning and that it can be used over paint and other coatings up to several millimeters in thickness).

ACFM is an electromagnetic method. A sensor probe is positioned on the surface to be examined and an alternating current is produced into the surface. In the absence of flaws, the alternating current creates an even magnetic field across the surface. Any defects if present will disturb the current, pushing it to flow around and beneath the fault; this triggers the magnetic field to develop non-uniform and sensors in the ACFM probe measure these field anomalies.

2.9.1 Ultrasonic Testing

Welds can be examined by the procedure of ultrasonic testing (UT) for example, the cracks in outer shell under the mean water level starting from the outside. UT can also be employed for inspection of internal cracks. The PoD curve for UT is expressed by

$$PoD(a) = 1 - \frac{1}{1 + \left(\frac{a}{X_o}\right)^b}$$

where, “a” is the depth of the crack. The parameters X_0 and b are calculated by curve fitting to experiments acknowledged in Nordtest: $X_0 = 0.410$ and $b = 0.642$.If no other documentation is specified, the PoD curves in Figure 9 can be used for inspection planning.

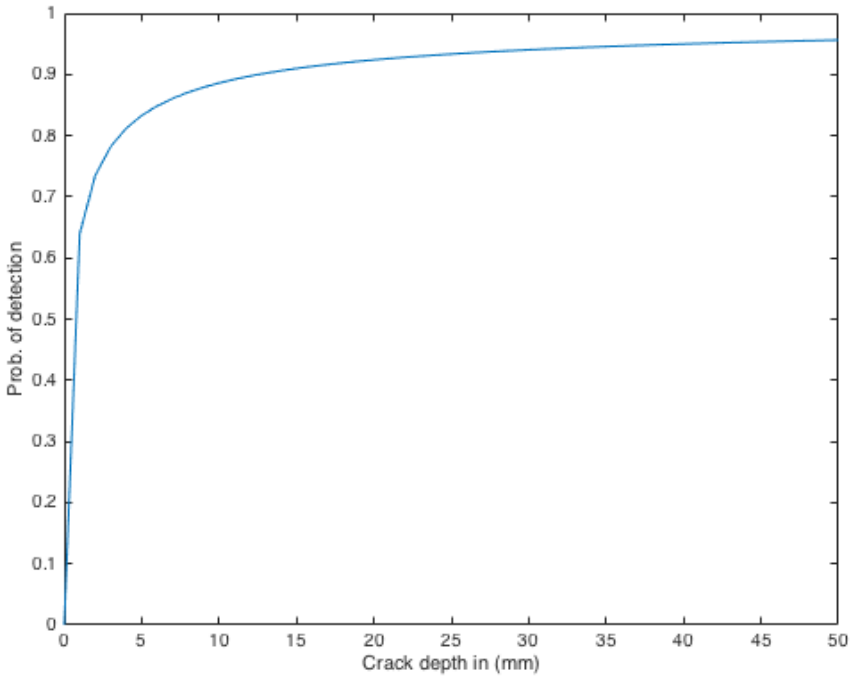

Figure 9 PoD curve for UT inspection (DNVGL-RP-0001)

2.9.2 Visual Inspection

There is not much info available associated to PoD data for Close Visual Inspection (CVI) based on test data. Supposing that the access is moderate, the cracks will be relatively deep already they can be spotted. Where the plate thicknesses are not large, this suggests that the cracks are grown throughout half the plate thickness. Then the time before the cracks develop through the thickness may be short. It is also perceived that the probability for detecting a crack that can be fixed by grinding is very low.

The PoD curves for visual inspection as shown in Figure 10 are established on judgement and not on tests. The reliability of a visual inspection is mainly dependent on cleaning of the examined area. The reliability of visual inspection is also dependent on category of fatigue crack. If the fatigue crack is alongside a weld toe without going through the plate thickness, it is considered to be more difficult to detect than a crack going through the thickness. Also the loading condition at the time of inspection is considered to effect the reliability of inspection as a through thickness crack exposed to membrane loading or bending loading tending to open the crack is easier to detect than a crack without external tensile loading. Thus the given

PoD curves for visual inspection should be employed jointly with engineering judgement reliant on actual inspection environments such as cleaning, light conditions etc. With a good cleaning high resolution image (HRI) photos are considered to qualify to the highest PoD curve in Figure 10. The section related to PoD curves is presented here in connection to the future work but is not included in the current work.

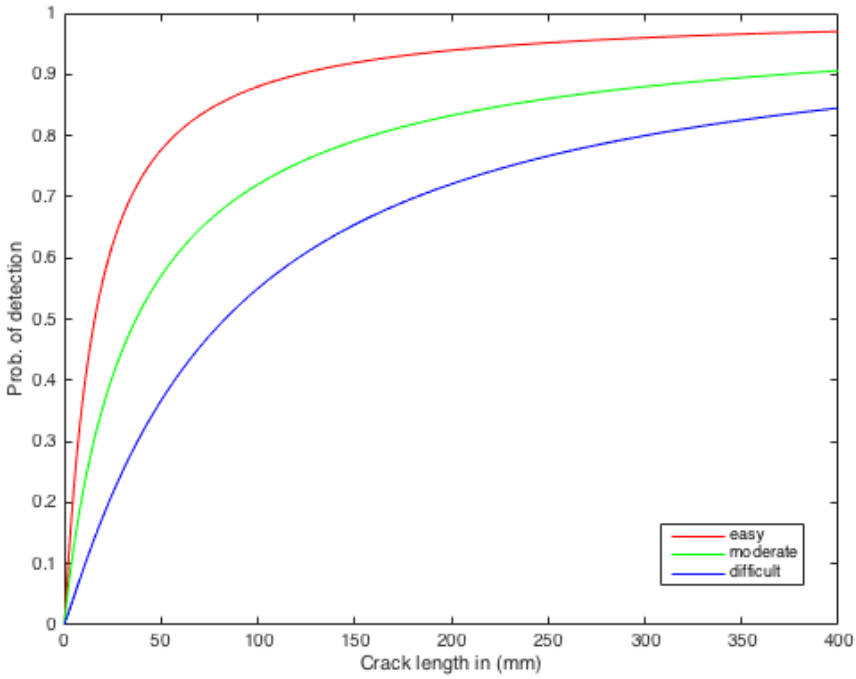

Figure 10 POD curve for visual inspection (DNVGL-RP-0001)

Table 2 PoD curves for visual inspections

Description	X_o	b
Easy access	15.78	1.079
Moderate access	37.15	0.954
Difficult access	83.03	1.079

Chapter 3

Introduction to Degradation Modeling

In this section different types of models will be discussed which can be used for degradation modelling and some of the models are compared with others on the basis of advantages / disadvantages.

According to Meeker and Escobar (1998), many failure mechanisms can be tracked to an underlying degradation process. Degradation ultimately leads to a weakness that can cause failure. In some reliability studies, it is likely to measure physical degradation as a function of time (e.g., tire wear). While in some other cases real physical degradation cannot be spotted directly, but measures of product performance degradation (e.g., power output) maybe available. Both types of data sets are generally stated as "degradation data". Figure 11 illustrates examples of three typical shapes of degradation curves in random units of degradation and time: linear, convex and concave. The horizontal line at degradation level 0.6 represents the level or approximate level at which failure would occur. A brief introduction about linear and convex degradation, as presented by Meeker and Escobar (1998), will be discussed in the following section.

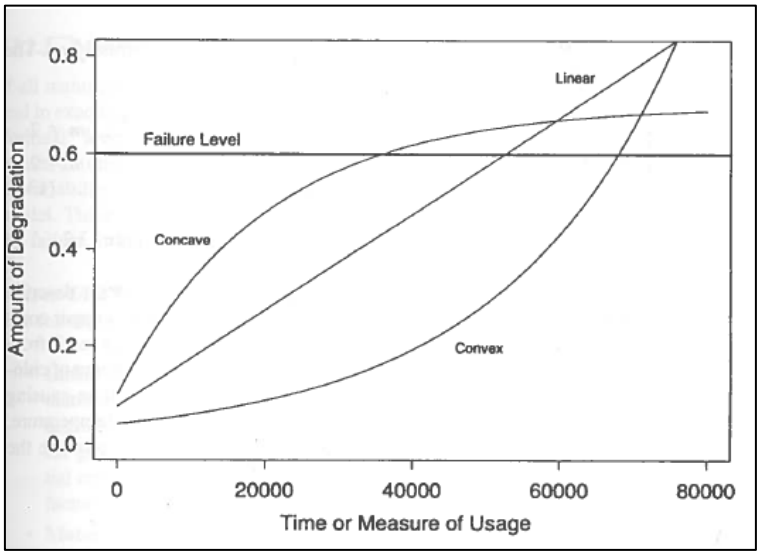

Figure 11 Possible shapes for univariate degradation(Meeker and Escobar, 1998).

3.1 Linear Degradation:

Linear degradation happens in some simple wear processes (e.g., automobile tire wear). For example, if *D(t)* is the amount of automobile tire tread wear at time t and wear rate is $Dt/dt = C$, then $D(t) = D(0) + C \times t$

The parameter $D(0)$ and C could be taken as constant for individual units, but random from unit-to-unit.

3.2 Convex Degradation:

Models for which the degradation rate increases with the level of degradation are, for example, used in modeling the growth of fatigue cracks. Let *a(t)* denote the size of a crack at time t. A simple version of the deterministic Paris-rule model (Dowling, 1993),

$$\frac{d\ a(t)}{dt} = C \times [\Delta K(a)]^m \qquad (1)$$

postulates a useful model for cracks within a certain size range. Here C and m are material properties and $\Delta K(a)$ (known as the "stress intensity rate function") is a function of crack size a, the range of applied stress, part dimensions, and geometry. For example, to model a two-dimensional edge-crack in a plate with a crack that is small relative to the width of the plate (say for example, less than 3%), $\Delta K(a) = Stress\sqrt{\pi a}$. $\frac{d\ a}{dN}$ is the crack growth rate or crack growth speed.

3.3 Models for Variation in Degradation and Failure Times:

According to Meeker and Escobar (1998), if we assume that all the manufactured components were alike, functioned under the same conditions and in the same operating environment and also every unit failed as it reached a particular "critical" level of degradation, then, according to simple deterministic models, all units would fail at exactly the same time. But always there is some variability in all of these factors of the model as well as in factors that are not in the model. Together all these factors produce variability in the degradation curves and in the failure times.

Unit-to-Unit Variability

The causes of unit-to-unit variability are discussed in detail as follows:

- **Initial conditions.** Individual units will differ with respect to the amount of material available to wear, initial level of degradation, amount of harmful degradation-causing material. The Paris model for development of fatigue cracks, with simulated variability in the size of the initial crack is shown in Figure 12., but all other factors and unit's Paris model characteristics are kept constant.

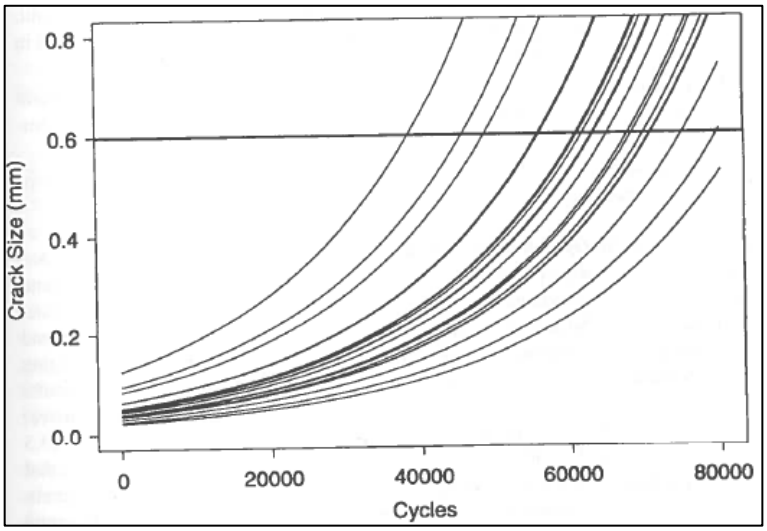

Figure 12 Plot of Paris model for growth of fatigue cracks with unit-to-unit variability in the initial crack size ao but with constant material parameters (C and m) and constant stress(Meeker and Escobar, 1998).

- **Material properties.** The Paris model for growth of fatigue cracks, enabling for unit-to-unit variability in the material properties parameters C and m and the size of the initial crack will cause the degradation curves to cross each other. The rate of growth in this case depends on C and m, which are different for unit to unit. This condition results in the form of crossing of the crack growth curves, that is distinctive of what is detected in actual fatigue testing.
- **Component geometry or dimensions.** Unit-to-unit variability in component geometry or dimensions can cause additional unit-to-unit variability, for example, in degradation rates (e.g., through the $\Delta K(a)$ function as observed in Paris-rule model equation).
- **Within-unit variability.** Frequently there will be spatial variability in material properties within a unit (e.g., defects).

Variability Due to Operating and Environmental Conditions

The rate of degradation will vary for different operating and environmental conditions. For example, $K(a)$ in the Paris model depends on the amount of applied stress and the Paris parameters can depend on temperature. In laboratory fatigue tests, the stress is either fixed or change in a systematic way(e.g, to keep $K(a)$ nearly constant as a increases. While in real operation of the most of the components, stress can be a complex function over time. These deviations can be defined by a stochastic process model. Figure 13, illustrates the Paris model with degradation rate varying due to variations in stress that might have been caused, for example, by variation in driving conditions encountered over time, by an automobile. Also in some applications, shocks or changes in environmental conditions that occur randomly in time can dominate other sources of variability in a failure-causing process (Meeker and Escobar, 1998).

3.4 Limitations of Degradation Data

Physical degradation or performance degradation, both are natural characteristics to measure for many testing processes (e.g., monitoring crack size of a specimen exposed to stress cycling or power output of an electronic device). However frequently, the degradation measurement of a unit involves destructive inspection (e.g., destructive strength tests) or disruptive measurement (disassembly and reassembly of a motor) that has the potential to change the degradation process. In these circumstances one can take only a single measurement on each unit tested. It is only possible to obtain useful information from such data if a large number of units can be examined.

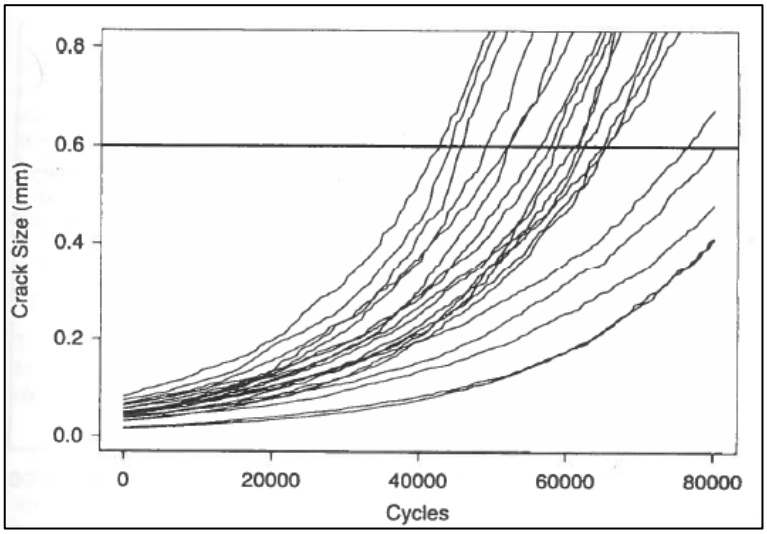

Figure 13 Plot of Paris model for growth of fatigue cracks with unit-to-unit variability in the initial crack size and material parameters C and m, and with a stochastic process model for the changes in stress over the life of the unit (Meeker and Escobar, 1998).

The benefits of degradation data can also be compromised when the degradation measurements are spoiled with large amounts of measurement error or when the degradation measure is not closely associated to failure. For example, when the degradation measurement is on performance degradation, rather than physical degradation, failure may arise for physical reasons that are not or cannot be detected directly (Meeker and Escobar, 1998).

3.5 Fatigue Crack Growth, A Fracture Mechanics Model

Cyclic fatigue involves the microstructural damage and failure of materials under cyclically fluctuating loads. However, the structural materials are seldom designed with compositions and microstructures optimized for fatigue resistance. Though metallic alloys are usually designed for strength (Ritchie, 1999). The fatigue damage progression of cyclically loaded structures can be explained by three phases, (1) crack initiation (2) crack propagation (3) unstable crack growth.

1) The crack origination/initiation stage starts with displacement movements inside grains and leads to micro-structural short cracks, which might be hindered at grain boundaries. But when the defects already exist inside the material (i.e., pores, inclusions), these defects can be seen as initial cracks without a crack initiation phase.
2) Once micro-cracks have been initiated and subsequently the cyclic loading is larger than the fatigue limit, these micro-cracks will grow to mechanically short cracks and

can be explained by fracture mechanics techniques. Crack propagation can be separated into short crack and a long crack part. Short crack propagation is expressed (a) by the effect of the cyclic plastic zone on the crack tip driving force, which does not allow the pure use of linear elastic fracture mechanics (LEFM) and (b) by the fact, that the plastically stimulated crack closure effect develops with raising crack length from 0% (no effect) to 100% (full crack closure effect). From this point on cracks can be defined as long cracks. If these cracks develop in a highly loaded notch field and the cyclic plastic zone is larger than about 1/10 of the crack length, elastic plastic fracture mechanics (EPFM) concepts must be used instead of linear elastic fracture mechanics.

3) At the end of fatigue life unstable crack growth occurs either in the case of brittle or of ductile damage of the structure. Different damage criteria can be defined like loss of stiffness, leakage, defined crack length and so on (Beier., et all, 2015).

3.6 Application of K to Design and Analysis

To use fracture mechanics practically, values of stress intensity factor K must be calculated for crack geometries that may exist in the structural components. K can be correlated to applied stress and crack length by the equation

$$\Delta K[a(N)] = F * \Delta S\sqrt{\pi a} \qquad (2)$$

- F is a dimensionless parameter or function depending on geometry and loading configuration.
- ΔS is the stress range (expressed in MPa)

The Value of F also depends on the ratio of the crack length to another geometric configuration, such as the member width or half width, b, as defined for the three cases in Figure 14. Hence, for a given type of loading, such as tension or bending

$$F = F\left(\text{geometry}, \frac{a}{b}\right) \qquad (3)$$

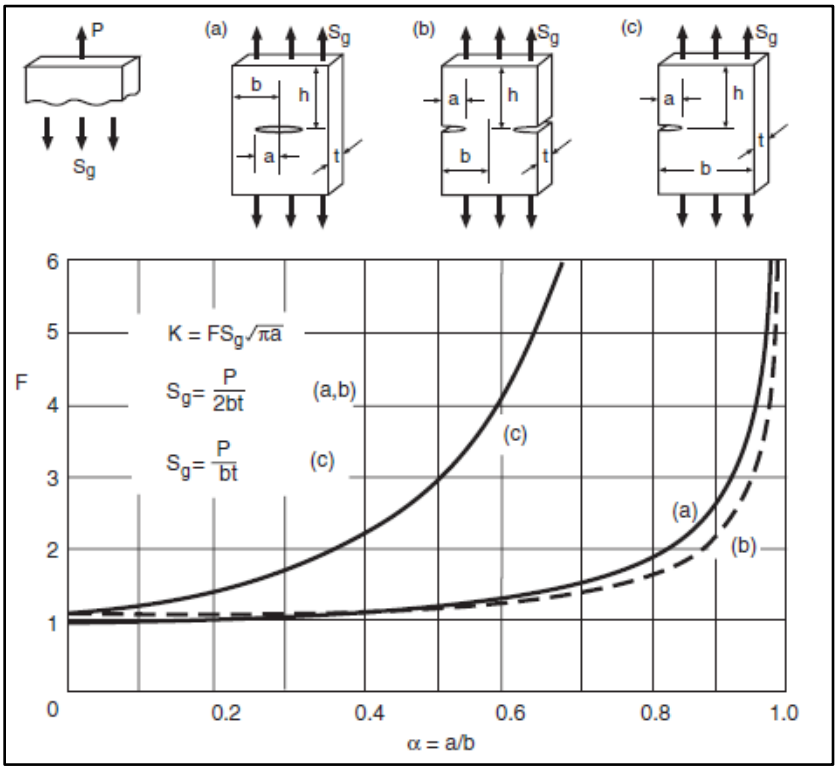

Figure 14 Stress intensity factors for three cases of cracked plates under tension (Dowling, 1998).

Values of K for small $^{a}/_{b}$ and limits for 10% accuracy for cracked plates under tension:

a) $K = S_g\sqrt{\pi a}$ $\quad (^{a}/_{b} \leq 0.4)$

b) $K = 1.12\ S_g\sqrt{\pi a}$ $\quad (^{a}/_{b} \leq 0.6)$

c) $K = 1.12\ S_g\sqrt{\pi a}$ $\quad \left(^{a}/_{b} \leq 0.13\right)$

Expressions for any $\alpha = {}^{a}/_{b}$

a) $F = \frac{1-0.5a+0.326a^2}{\sqrt{1-a}}$ $\quad (\frac{h}{b} \geq 1.5)$

b) $F = (1 + 0.122\ cos^4\ \frac{\pi\alpha}{c}\ \sqrt{\frac{2}{\pi\alpha}}\tan\frac{\pi\alpha}{2})$ $\quad (\frac{h}{b} \geq 2\ )$

c) $F = 0.265\ (1-\alpha)^4 + \frac{0.875+0.265\alpha}{(1-\alpha)^{3/2}}$ $\quad (\frac{h}{b} \geq 1)$

3.7 Cases of Special Interest for Practical Applications

Cracks with shapes that approaches a circle, half-circle or quarter-circle may occur as shown in the Figure 15. Especially half-circular surface cracks as in the parts (b) and (d) are

common. Assessment of stress intensities for these complex three-dimensional case is aided by the existence of an exact solution for a circular crack of radius a in an infinite body under uniform stress S.

$$K = \frac{2}{\pi} S\sqrt{\pi a} \qquad (4)$$

For embedded (internal) circular cracks, Figure 15(a) , this solution is still within 10% for members of finite size subject to the limits $a/t < 0.5$ and $a/b < 0.5$. For half-circular surface cracks or quarter-circular corner cracks, and for a values that are small compared to the other dimensions, the stress intensities are elevated compared to Eq. 4 by a factor around 1.13 or 1.14, giving F values as shown in Figure 15 for cases (b), (c) and (d). These F values particularly apply for points where the crack front intersects the surface, where k has its maximum value. They may be applied for either tension or bending, with 10% accuracy, within the limits implied. The factors of 1.13 1nd 1.14 on K compared to the circular crack case are analogous to the previously discussed free surface factor of 1.12 for cracks in flat plates.

Case	**S_t**	**S_b**	**F for small a**	**Limits for $\pm$10% on *F***
(a)	$\frac{P}{4bt}$	–	$\frac{2}{\pi} = 0.637$	$\frac{a}{t}, \frac{a}{b} < 0.5$
(b)	$\frac{P}{2bt}$	$\frac{3M}{bt^2}$	0.728	$\frac{a}{t} < 0.4, \frac{a}{b} < 0.3$
(d)	$\frac{P}{bt}$	$\frac{6M}{bt^2}$	0.722	$\frac{a}{t} < 0.35, \frac{a}{b} < 0.2$
(e)	$\frac{4P}{\pi d^2}$	$\frac{32M}{\pi d^3}$	0.728	$\frac{a}{d} < 0.2 \; or \; 0.35^*$

Note: *Different limits for tension or bending, respectively.

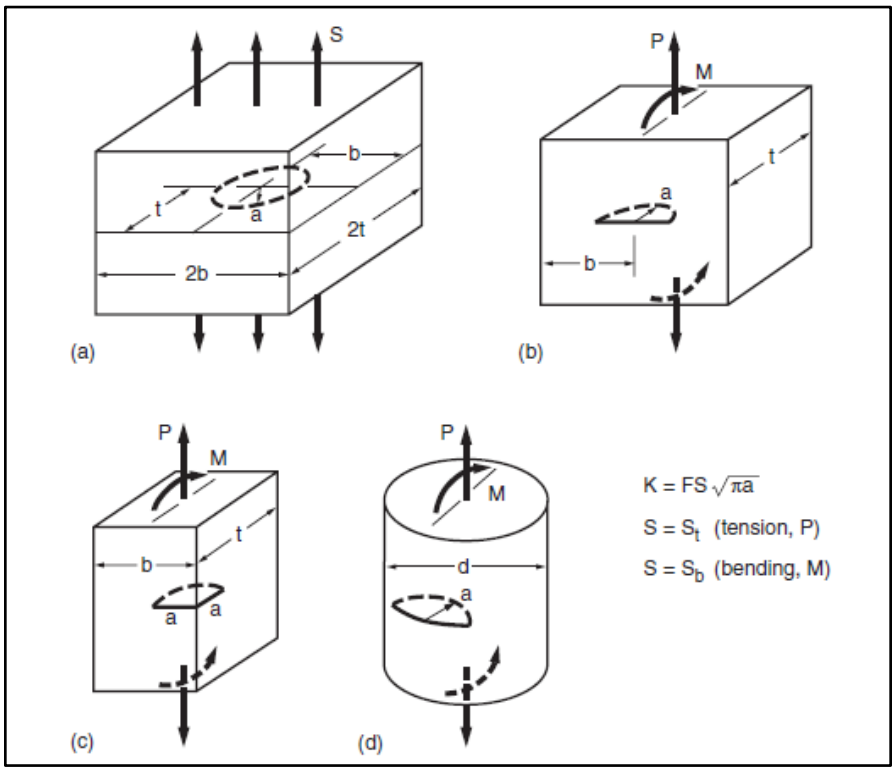

Figure 15 Stress intensity factors for (a) an embedded circular crack under uniform tension normal to the crack plane and related cases (b) half-circular surface crack (c) quarter-circular corner crack, and (d) half-circular surface crack in a shaft (Dowling, 1998)

Condition-based maintenance and condition-based replacement, which is discussed in detail by Rausand and Høyland (2004), will be briefly presented in the following section.

3.8 Condition Based Maintenance:

Generally, the maintenance is described as the combination of all technical and administrative actions, intended to retain an item in, or restore to, a state in which it can perform a required function (IEC 60050-191:2001). There are two types of maintenance commonly used in practice, preventive maintenance and corrective maintenance. Preventive maintenance is carried out at predetermined intervals or according to prescribed criteria and intended to reduce the probability of failure or the deterioration of the functioning of an item (IEC 60050-191:2007). Corrective maintenance is carried out after fault recognition and intended to put an item into a state in which it can perform a required function (IEC 60050-191:2007). Preventive maintenance includes different types of maintenance plans. The common preventive maintenance practices are time based and condition based.

Condition based maintenance is a type of preventive maintenance based on the assessment of physical condition. The condition assessment may be by operator observation, conducted

according to a schedule, or by a condition monitoring of system parameters (www.electropedia.org). The variables can be physical variables (e.g., thickness of material, erosion percentage, temperature, or pressure), system performance variables (e.g., quality of produced items or number of rejected items), or variables related to the residual life of the system. In the last case, the expression predictive maintenance is often used rather than condition based maintenance.

The CBM approach necessitates a monitoring system that can deliver measurements of selected variables, and a mathematical model that can forecast the behavior of the system deterioration process. The type of maintenance action, and the date of the action are decided based on an analysis of measured values. A decision is taken when a measurement (of a variable) passes a predefined threshold value. The threshold values make it possible to divide the system state space into different decision areas, where each area characterizes a specific maintenance decision. This type of maintenance strategy is called a control limit strategy and is only relevant for systems with an increasing failure rate.

3.9 Condition-Based Replacements

Let $X(t)$ be a random variable describing the deterioration of the item at time t, and assume that $X(t)$ is measured on a continuous scale. The item is supposed to be deteriorating in such a way that $X(t)$ is non-decreasing as a function of t. The item is inspected and the deterioration $X(t)$ is measured at the specific points of time t_1 and t_2 ….. The variable $X(t)$ is only measured at the inspections at times t_1 and t_2 …., and not between these points of time. When a measurement $X(t) \geq X_p$, the item should be preventively replaced. If a measurement $X(t) \geq X_c$ ($>X_p$), the item is in a failed state and has to be correctively replaced. A failure is not identified instantaneously when $X(t)$ passes the failure limit X_c. The failure will be detected at the first inspection after $X(t)$ has passed X_c. The corrective replacement cost will be significantly higher than the preventive replacement cost. After a replacement (preventive or corrective) the item is assumed to be as good as new.

Let us consider a simple deterioration (wear) example of the brake pads on the front wheels of a car and let $X(t)$ be the wear (the reduction of the thickness of the brake pads) at time t, where t is the number of kilometers driven since the brake pads were new. The wear $X(t)$ is measured (controlled) when the car is at the garage for service at regular intervals of length (e.g., 15000 km). The brake pads should be preventively replaced when the wear is greater

than X_p. If the wear exceeds than X_c, the brake effect is reduced, the pad holders will make scratches in the brake discs, and the discs will have to be replaced. The cost of this replacement will be significantly higher than the cost of only replacing the brake pads. In addition to this the risk cost due to reduced braking efficiency should be considered also.
According to van Noortwijk 2009, for engineering structures and infrastructures, it is more remarkable to base a failure model on the physics of failure and characteristics of the operating environment. So, it is suggested to model deterioration in terms of a time-dependent stochastic process.

3.10 Stochastic deterioration processes

For modeling stochastic deterioration, we can use either a failure rate function or a stochastic process such as Markov process, Brownian motion with drift, and non-decreasing jump process (gamma process is a special case of this). According to Singpurwala, (1995) "a more appealing approach would be to choose a model based on the physics of failure and the characteristics of the operating environment". Dynamic environments, such as applied stresses and loads, influence failure and vary over time. So, it is suggested to model deterioration in terms of a time-dependent stochastic process $\{X(t), t\geq 0\}$, where $X(t)$ is a random quantity for all $t\geq 0$.

3.10.1 Markov processes

Barlow and Proschan (1965) presented a model where they suppose that deterioration can be modelled by a Markov process. A Markov process is a stochastic process with the property that, given the value of $X(t)$, the values of $X(T)$, where $T>t$, are independent of the values of $X(u)$, $u<t$. It means that conditional distribution of the future $X(T)$, given the present $X(t)$ and the past $X(u)$, is independent of the past. The classes of Markov processes which are useful for modeling stochastic deterioration are discrete-time Markov processes having a finite or countable state space (named Markov chains) and continuous-time Markov processes with independent increments. An example of a stochastic process with Markov is Brownian motion with drift (also called Gaussian or Wiener process), the compound Poisson process, and the gamma process. The supposition of independent increments is more restricting than the Markov property. Because the increment $X(T) - X(t)$ is independent of the $X(t)$ and $X(T) =$

X(t) + [X(T) -X(t)], the stochastic process *{X(t), t≥0},* is Markovian. So the damage growth with independent increments leads to a Markov property.

The Brownian motion with drift is a stochastic process *{X(t), t≥0},* with independent, real-valued increments and decrements having a normal distribution with mean μt and variance $\partial^2 t$. The compound Poisson process is a stochastic process with independent and identically distributed jumps which occur according to a Poisson process. A gamma process is a stochastic process with independent, non-negative increments having a gamma distribution with an identical scale parameter. Like the compound Poisson process, the gamma process is also a jump process. According to Singpurwalla and Wilson 1998, the key difference between these two jump processes is that the Compound Poisson process have a finite number of jumps in finite time intervals, while gamma processes have an infinite number of jumps in finite time intervals. Compound Poisson processes are appropriate for modeling usage such as damage due to irregular shocks and the gamma processes are suitable for defining gradual damage by continuous use.

3.10.2 Gamma Processes

According to van Noortwijk (2009), a gamma process is the special type of stochastic process having independent, non-negative increments. Abdel-Hameed (1975), firstly proposed the gamma process as an appropriate model for deterioration occurring random in time. He has called this stochastic process as the "gamma wear process". The benefit of modelling deterioration processes through gamma process is that the vital mathematical calculations are somewhat straightforward. The gamma process is appropriate to model gradual damage monotonically accumulating over time in a series of small increments, for example wear, fatigue, corrosion, crack growth, erosion, consumption, creep, swell, degrading health index, etc.

Definition of a non-stationary gamma process

If X is a random quantity which describes the deterioration of an item, the gamma process will have the following characteristics:

Random quantity X has a gamma distribution with shape parameter $\mathcal{V} > 0$ and scale parameter $\mathcal{U} > 0$ and the probability density function of X is given by

$$\mathrm{Ga}(x|\mathcal{V},\mathcal{U}) = \frac{\mathcal{U}^{\mathcal{V}}}{\Gamma(\mathcal{V})} x^{\mathcal{V}-1} e^{-\mathcal{U}x} \qquad (5)$$

Where, $\Gamma(a) = \int_{z=0}^{\infty} z^{a-1}\, e^{-z}$ is the gamma function for $a > 0$.

Additionally, let $\mathcal{V}(t)$ be a non-decreasing, right continuous, real valued function for $t \geq 0$, with $\mathcal{V}(0) \equiv 0$. The gamma process with shape function $\mathcal{V}(t) > 0$ and scale parameter $\mathcal{U} > 0$ is a continuous-time stochastic process *{X(t), t≥0}*, with the following properties:

1) $X(0) = 0$ with probability one;
2) $X(\tau) - X(t) \sim \mathrm{Ga}\,(\mathcal{V}(\tau) - \mathcal{V}(t), \mathcal{U})$ for all $\tau > t \geq 0$, where $X(\tau) - X(t)$ is the increment of the process;
3) *X(t)* has independent increments.

Mean and Variance of gamma process

Let *X(t)* denote the deterioration at time t, $t \geq 0$, and let the probability density function of *X(t)*, in accordance with the definition of the gamma process, be given by

$$\mathrm{f}_{X(t)} = \mathrm{Ga}(x|\mathcal{V}(t),\mathcal{U})) \qquad (6)$$

with expectation and variance

$$E(X(t)) = \frac{\mathcal{V}(t)}{\mathcal{U}}, \qquad \mathrm{Var}(X(t)) = \frac{\mathcal{V}(t)}{\mathcal{U}^2}. \qquad (7)$$

The coefficient of variation is defined by the ratio of the standard deviation and the mean, that is

$$\mathrm{CV}\big(X(t)\big) = \frac{\sqrt{Var\,(X(t))}}{E(X(t))} = \frac{1}{\sqrt{\mathcal{V}(t)}} \qquad (8)$$

Which decreases as time increases. While on the other hand the ratio of the variance and the mean equals $1/\mathcal{U}$ and therefore does not depend on time.

Simulation of gamma processes

For sampling independent gamma-process increments, there are basically two simulation methods: gamma-increment sampling and gamma-bridge sampling. A better methodology to simulate gamma process is the simulation of independent increments with respect to very small units of time. In this way, defining the time grid is the first step as follows: $0, t_1, t_2, \ldots\ldots\ldots, t_{n-1} t_n$, where $t_i = (i\,/\,n)t$ for some $t > 0$ and $i = 0, \ldots\ldots, n$. The next step is simulating sample paths of the gamma-process by randomly drawing independent increments $X(t_1), X(t_2) - X(t_1), \ldots\ldots\ldots, X(t_n) - X(n-1)$ using Monte Carlo simulation.

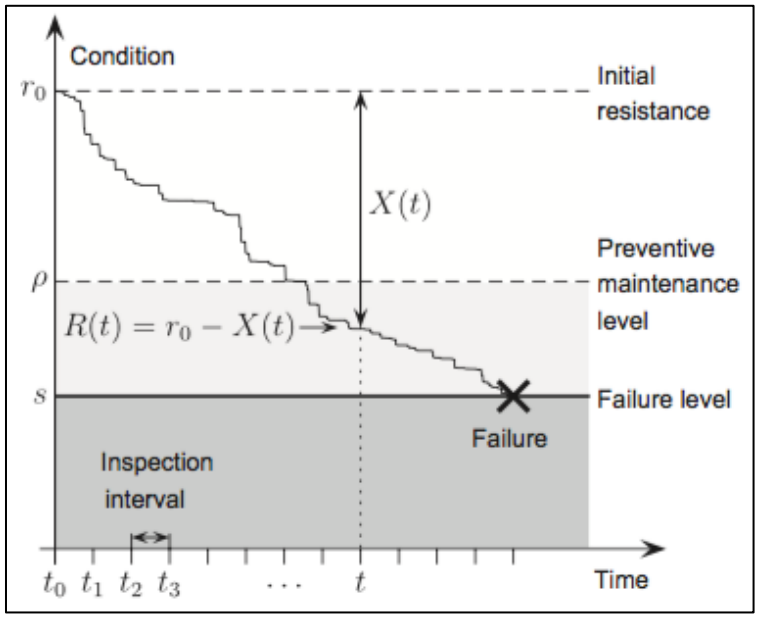

Figure 16 Basic condition-based maintenance model with gamma process deterioration(van Noortwijk,2009)

Chapter 4

Brief Presentation of NOWIcob Model

4.1 Introduction

This section explains the NOWIcob model (which has been developed in the NOWITECH WP5 and FAROFF) and is mainly based on a report (Hofmann et al.,(2015)). NOWIcob is an analysis tool that can be utilized for decision support for different features of offshore wind farm operation and maintenance and logistics strategies. It simulates the maintenance activities and related logistics of an offshore wind farm over a given number of years to assess key performance parameters such as wind farm availability and operation and maintenance costs. This model has two potential user groups, researchers and wind farm developers/operators.

For the research aspect, this model can be utilized for the analysis of various operations and maintenance (O&M) approaches, which includes strategies for logistic support and wind turbine access. The wind farm developers can employ NOWIcob for cost-benefit assessment of different technical solutions for an offshore wind farm project. This model can also assist as decision support tool for decision problems for example, what kind of crew transfer vessels could be used, where to base the maintenance locations or if the benefits of improvement in condition monitoring will counterbalance the cost.

4.2 General Description of the Model

The core purpose for the development of NOWIcob model is the evaluation of the operation and maintenance strategy for offshore wind farms. This strategy involves all the decisions on convenient options in an offshore wind farm project which effect the operation and maintenance cost and the secondary cost related to loss of income due to downtime in case of failure of the system.

This model is based on the time-sequential (discrete-event) Monte Carlo simulation practice, in which the maintenance operations in an offshore wind farm are simulated for a number of

years of its operational lifetime with an hourly resolution. NOWIcob also contains the possibility to deliberate future vessel models for example mother/daughter vessel combinations or crew transfer vessels that are offshore for several shifts. The offshore maintenance tasks greatly depend on weather, so the uncertainty of weather is deliberated in NOWIcob by employing the Monte Carlo simulation approach with a weather model creating new, characteristic weather time series for each Monte Carlo iteration. Due to the uncertainties in the generated series, several Monte Carlo iterations should be executed for each case. This also permits the results provided by the model to be shown as histograms approximating probability distributions. The results comprise numerous performance factors, for example availability of the wind farm, the operation and maintenance cost and the revenue of the wind farm project (Figure 17). It is possible to model the whole operational lifetime (for example commissioning to decommissioning) by performing simulations of the wind farm and also to calculate the performance parameters as the net present value, e.g., of the profit.

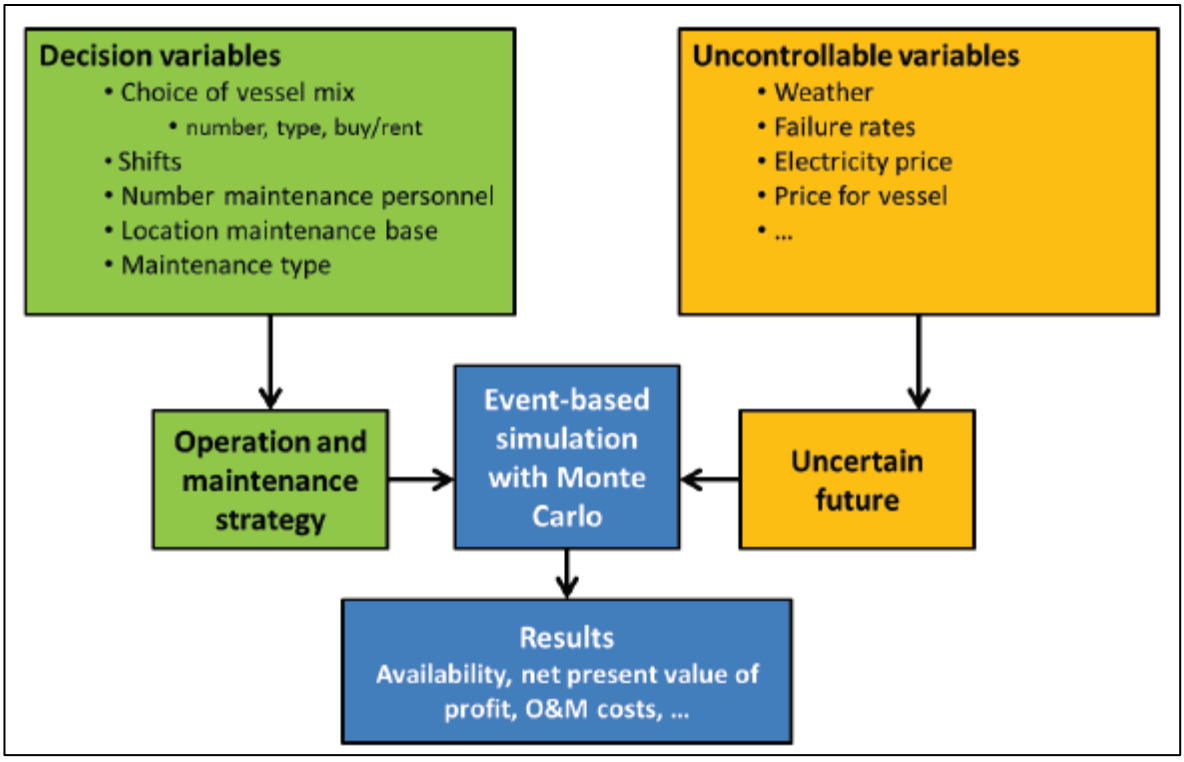

Figure 17 Decision variables and uncontrollable variables (Hofmann, et al.,2015).

4.3 Input-Output Structure of the Model

Generally, the process flow of the model can be distributed into four logical steps:

1) Input data
2) Weather simulation
3) Maintenance and logistics
4) Results

This model is executed in MATLAB, but user interfaces for inserting input data and for looking the results are in the form of Excel sheets. The basic flow pattern of the model established on these steps is presented in Figure 18.

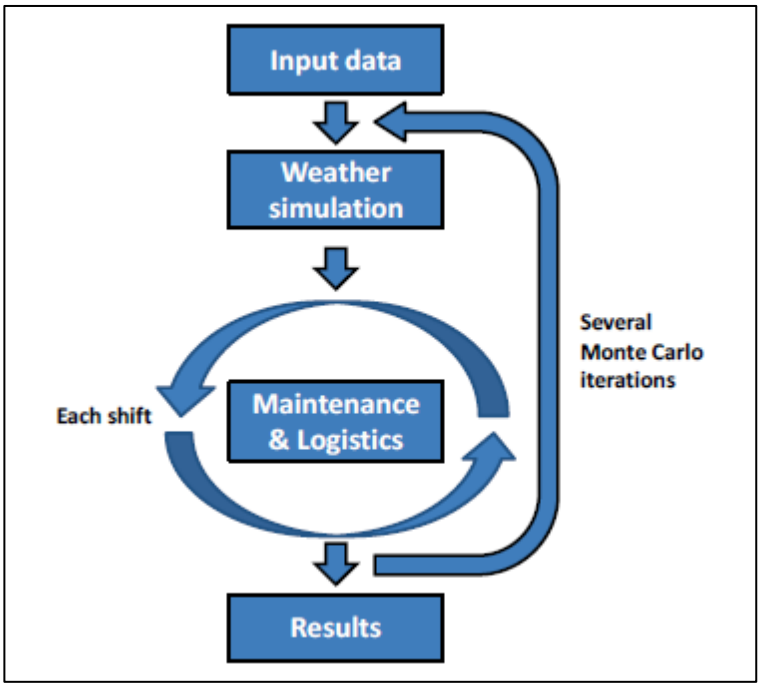

Figure 18 Simplified flow scheme of the model (Hofmann, et al.,2015).

The input data for each exclusive case is imported and pre-processed. Secondly the weather is simulated for each Monte Carlo iteration for the entire lifetime of the wind farm. The fundamental part of the model is the maintenance tasks and associated logistics that are simulated throughout the pre-defined simulation period.

4.4 Input Data

The data input in NOWIcob model is controlled through two excel sheets, where one encloses basis data and the other has case-specific data. In addition to this, a text file with historical weather time series is required. The basis data comprises all information that can be reclaimed in many case-specific set ups. Examples of this basis data are electricity price scenarios and different type of vessels. While the case specific data mentions directly to the basis data, a

classic methodology of formulating the data for the model is first to specify the basis data and later the case specific data. The weather data is represented by a data time series and is saved in separate text files.

4.5 Input Parameters

For each specific wind farm, examples of some important input parameters that must be specified are:

- Simulation period in years
- Weather data file as a time series of various weather parameters (i.e., wind speed and major weave height)
- Number of Monte Carlo iterations
- Working hours for each shift
- Electrical loss
- Number of daily shifts

Some other parameters which are not listed here, must also be specified, such as the data about main components of the wind farm.

Maintenance activities are the set of operations that must be executed to complete the maintenance task (Predetermined preventive maintenance tasks and Corrective and condition-based maintenance tasks). Each maintenance action involves at least one main operation step and also in addition a pre-inspection can be stated. Predetermined preventive maintenance tasks are executed on a time plan can be specified with some specific parameters. In response to some random failures the corrective maintenance tasks can be executed, while the tasks based on condition monitoring techniques can be performed as condition-based maintenance tasks while mentioning specific input data. The information about vessels can also be specified for example number of vessels, vessel type, day rate and other important information.

4.6 Prioritization of Maintenance Tasks and Vessels

Several maintenance tasks can be planned for a shift and if many of them are competing for limited maintenance resources, then a priority can be set for the most important one to be

executed first. The priority criteria have been set on three basic rules. By default, the model gives priority to maintenance tasks after the following order:

1) Type of maintenance task:
    I. Corrective maintenance is on highest priority
    II. Condition-based maintenance comes second
    III. Thirdly time-based maintenance
2) Whether the maintenance task has already started:
    I. Maintenance tasks that are already started are on higher priority
    II. While the tasks not yet started will be handled secondly
3) Whether an ordered vessel is required for performing that task
    I. If the maintenance task demands ordering of a vessel (jack-up vessels), they are considered more important
    II. While the maintenance tasks with no requirement of vessel are on second priority.

But also for special situations, a different priority can be set. So the model is quiet flexible for case to case.

4.7 Condition Based Maintenance

Condition-based maintenance is expressed in the model as follows. For each failure category (component/failure model), it can be indicated whether condition monitoring is able to give an early warning for a potential failure or not. If this is the case, the overall probability that a prospective failure is detected and a warning is given (P_{det}) must be specified, together with the pre-warning time (T_{det}). The pre-warning time is the number of days between the warning and when the failure would have been occurred if the warning had not been given. This pre-warning time is an input parameter specified either as a fixed number (average pre-warning time), so that the time available for performing the condition based maintenance task is always the same, or as a stochastic variable with a normal distribution or a triangular distribution.

The two quantities, P_{det} and T_{det}, are reliant on the degradation process $X(t)$ (fast or slow degradation, linear or exponential degradation), the inspection approach (how often the inspections are carried out and type of inspection method employed). The later also involves

the effectiveness of the inspection method that could be stated as the Probability of Detection (POD), which is the probability to detect a flaw of a given size which can develop to a failure (for example a crack leading to fracture) when the inspection/detection approach is applied once.

Assuming that inspections are carried out according to a schedule with time intervals (T) between each inspection and also assuming that these intervals are shorter than the time interval between the earliest point in time when the potential failure/flaw can actually be detected and the time when failure will happen (the PF-interval, T_{PF}), then T_{det} is shorter than T_{PF}. This concept is illustrated in Figure 19 but not modelled yet explicitly in the NOWIcob. So the effects of different degradation speed, different inspection intervals and strategies and different detection capabilities of various inspection methods on pre-warning time and overall detection probability must be incorporated in the values of p_{det} and T_{det}. T_{PF} is the theoretical maximum pre-warning time that can be reached with condition-based maintenance, with the aid of continuous monitoring/continuous inspections and POD of 100% as soon as the potential failure becomes detectable, we could assume $T_{det} = T_{PF}$ and p_{det} is 100%.

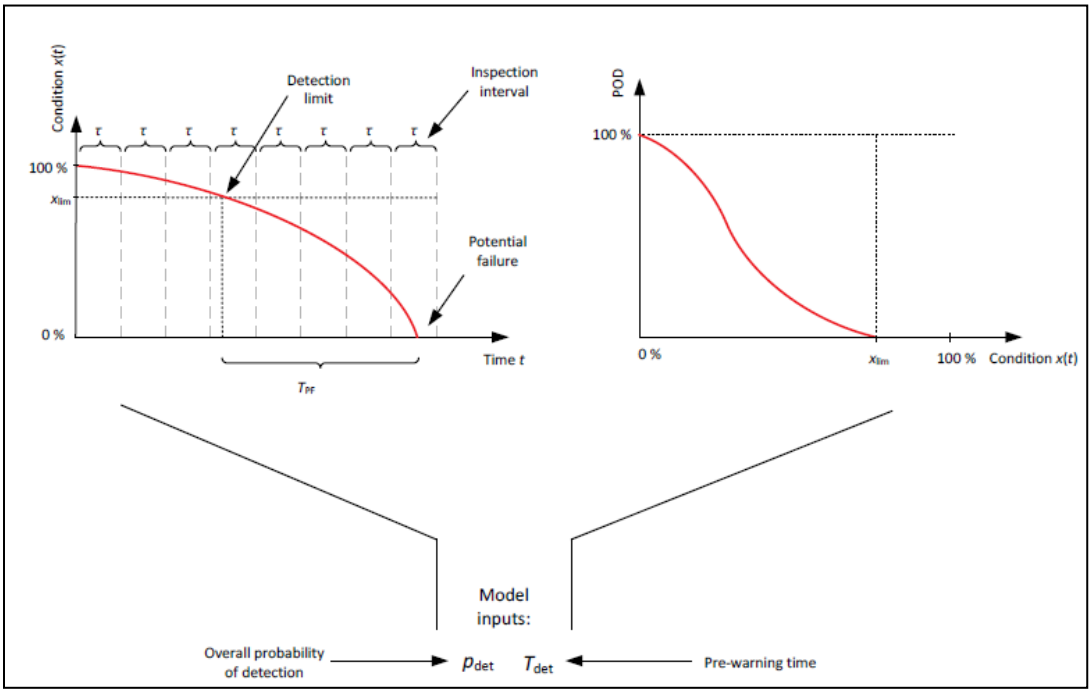

Figure 19 Conceptual illustration of degradation of the condition of a component (left) and the probability of detection of this degradation (right) together with the input parameters representing these processes in the O & M strategy model (Hofmann, Sperstad and Kolstad, 2014)

The objective of the project is to model the degradation explicitly and try to find the average pre-warning time T_{det}. If the maintenance will be carried out during the time window T_{det}, then the condition-based maintenance shall be performed rather than corrective maintenance (in case of failure). The time to repair T_R, the time before the maintenance task is completed, is generated implicitly and stochastically in the simulations. This means that for each potential failure in the model, if $T_R<T_{det}$ then there is sufficient time to perform condition-based maintenance before the occurrence of failure and if $T_R>T_{det}$, (means time to repair is greater) which implies that with this modelling approach the component will run to failure and a corrective maintenance operation will be performed.

Different alternatives to operate the turbine, in case if condition-based maintenance is not feasible and cannot be completed in time, (e.g., shut down of turbine before leading to failure if a potential failure has already been detected) is not integrated in the model. If the potential failure is not detected at all, this will also lead to failure and ultimately to corrective maintenance task. The possible outcomes of the simulation are illustrated in the Figure 20.

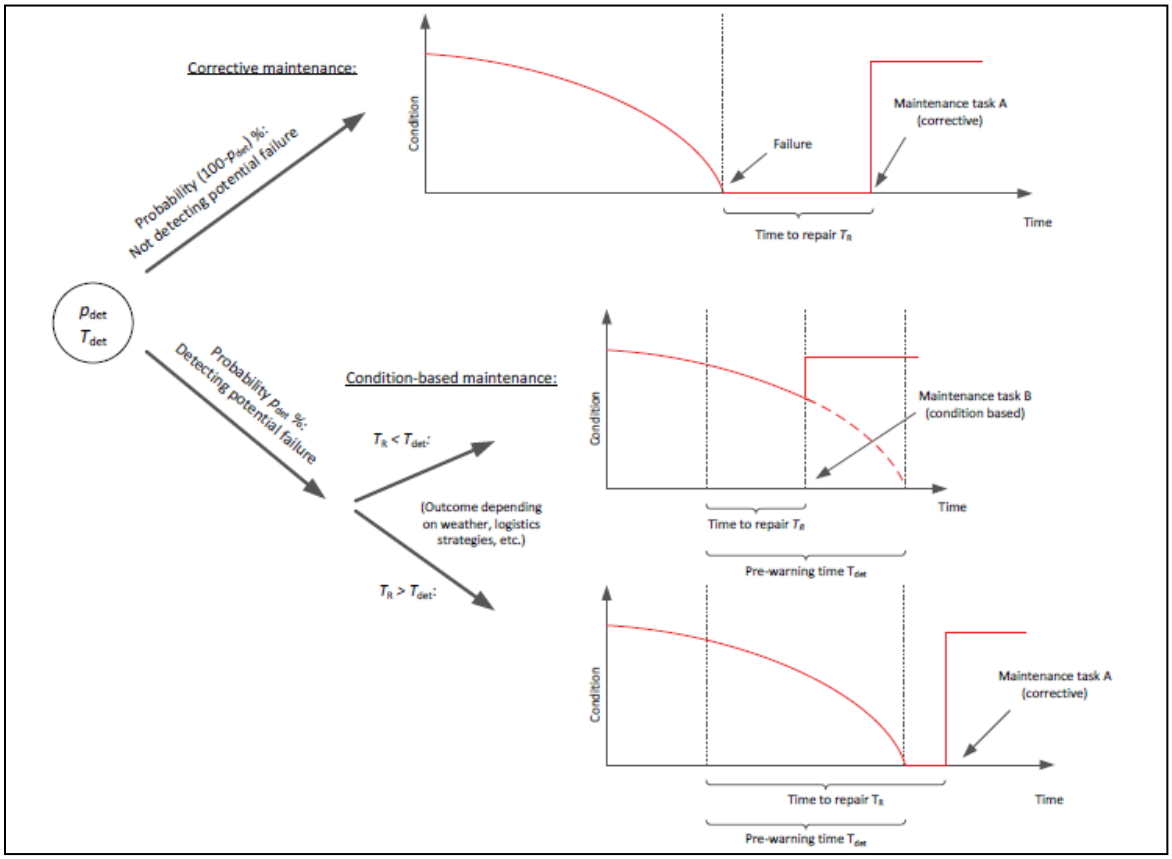

Figure 20 Possible outcomes in the simulation of condition monitoring (Hofmann, Sperstad and Kolstad, 2014)

The NOWIcob model developed at SINTEF Energy Research includes in the current version a very simple "module" for condition based maintenance. As illustrated in the figure above the input required by NOWIcob is P_det (= overall probability of detection, given an underlying degradation/failure process and an inspection strategy) and T_det (= Pre-warning time, i.e. time interval of getting a warning from the inspections or condition monitoring before the failure actually happens, and again: given an underlying degradation/failure process and an inspection strategy). This means that degradation is not explicitly modelled in NOWIcob. P_det and T_det can be (deterministic) mean values or stochastic/random variables represented by any probability distribution. Good input values for P_det and T_det might be difficult to estimate, because in reality they are usually not directly observable. However, they could be estimated from "observable" quantities when we know what the underlying failure mechanism is (e.g. crack growth). Current work is now to demonstrate how P_det a and T_det can be estimated based on an underlying crack growth model, and an inspection strategy. Crack growth models (e.g. Paris law) is one of the degradation models that we consider for exemplifying the loose integration approach.

4.8 Results

The results can be presented in the form of following categories:

- Energy based availability
- Electricity production
- Net present income
- Net present O&M cost
- Net present value of profit

There are several interesting aspects of the model which are not described here because they are not directly related to the scope of the present thesis work. A test data set has been provided with the NOWIcob model to check the output and get familiar with the input parameters of the model. So this “TEST” data set has been executed and the result of operation and maintenance cost with sub-categories is presented in Figure 21.

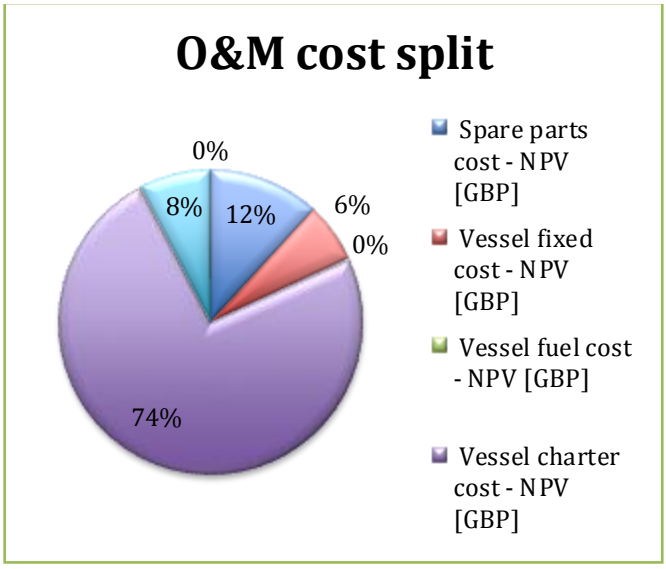

Figure 21 Representation of operation and maintenance cost split from the NOWIcob model (Hofmann, et al.,2015).

Chapter 5

Methodology

Monte Carlo Approach

Monte Carlo was used for simulating degradation and a condition-based maintenance strategy with regular inspections, preventive maintenance (when the degradation is above the acceptance limit), and corrective maintenance when failure occurs. For this purpose, MATLAB (Mathworks, 2016) scripts were created to carry out the simulations (Appendix 1&2).

Degradation Modeling

Out of the models presented in the previous section, two models were used to analyze the degradation of offshore monopile structures:

i) Fatigue crack growth model on Paris law
ii) Gamma Process.

A comprehensive emphasis has been put on to the crack growth model.

Estimation of Stresses

i) The hot spot stress ranges at tower bottom and mud line scaled to 20 years of lifetime has been employed from Ziegler et al., (2016) (to be published).
ii) The stresses have been approximated triangular distribution.

Introducing Inspections

Inspections are introduced to detect the crack size to check if it is large enough to be detected by condition monitoring approaches. Once detected, if it has reached the limit to carry out preventive maintenance or otherwise if it has crossed this limit then the component must be replaced by corrective maintenance.

Assumptions

Some assumptions are made on the stresses, i.e., the stress values are triangular distributed around 0-100mm with the parameters a=0, b=0, c=100. Where a and c are lower and upper limit parameters and b is the peak location parameter. Also for the critical crack size, which is taken equal to the thickness of the material.

Chapter 6

Simulation Results for Degradation Modeling

For the two models that were selected, Fatigue Crack Growth Model and Gamma Process, the results are presented in the following section.

The deterministic solution (or closed form solution) to the resulting differential equation is then given by the following expression

$$a(N) = \text{ao}^{(1-m/2)} + (1 - m / 2) \times C \times (S\sqrt{\pi})^m \times N \qquad (1)$$

One way to model the crack growth step by step (incorporating Monte Carlo Simulations) and the equation (1) will take the form,

$$\frac{\Delta a}{\Delta N} = C .\{S\sqrt{\pi . a(N)}\}^{m*} \qquad (2)$$

where, $\frac{\Delta a}{\Delta N}$ is the crack growth.

Now to calculate the crack growth step by step (assuming that ΔN = 1), one can write the equation (2) in the following way,

1st step, $a\ (N = 1) = a(N = 0) + C .\{S\sqrt{\pi . a(N = 0)}\}^{m*}$, ($\frac{\Delta a}{\Delta N}$ for first cycle)

2nd step, $a\ (N = 2) = a(N = 1) + C .\{S\sqrt{\pi . a(N = 1)}\}^{m*}$, ($\frac{\Delta a}{\Delta N}$ for second cycle)

3rd step, $a\ (N = 3) = a(N = 2) + C .\{S\sqrt{\pi . a(N = 2)}\}^{m*}$, ($\frac{\Delta a}{\Delta N}$ for third cycle)

The calculations for next steps can be written in the same way.

Table 3 Parameters used in the fatigue crack growth model

Parameters	Unit	Range used in the model	Reference
Initial crack size a_c	mm	0.1-2	DNV-OS-J101
Stress Range S	MPa	0-100	
Material parameter C	$\frac{m\ /\ cycle}{(MPa\sqrt{m})^{m*}}$	1.10^{-11}	DNV-OS-J101
Material parameter m	-	3	DNV-OS-J101
Parameter F	-	1-1.12	Dowling 1998

6.1 Results of Fatigue Crack Growth Modelling for an Offshore Monopile Structure

To analyze the effect of variation in parameters presented in the Paris Model, plots has been drawn and are presented accordingly.

- Paris Model for growth of fatigue cracks with variable F parameter but with constant material parameters (C and m) and constant stress S Figure 22.

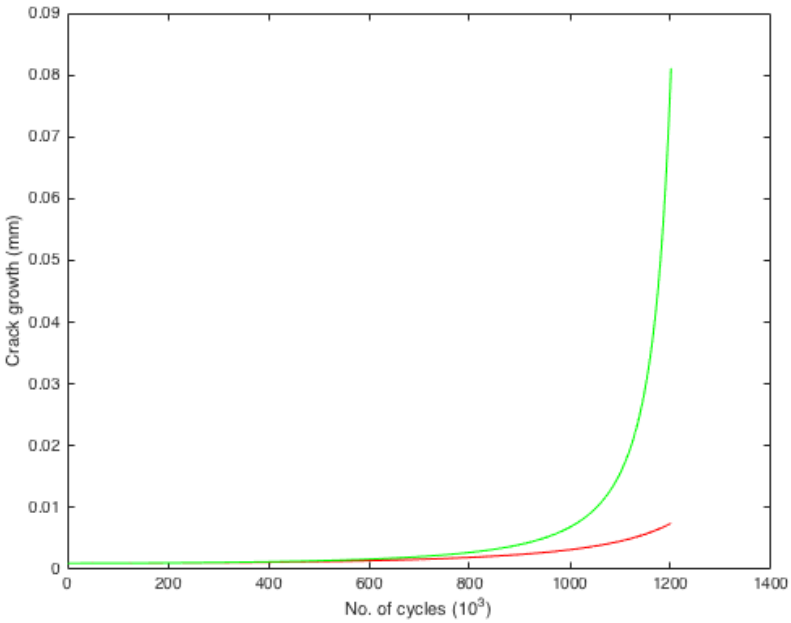

Figure 22 Plot of Paris model for two values of F(1, 1.12 respectively)

- Plot of Paris model for growth of fatigue cracks with variable initial crack size but with constant material parameters (C & m) and constant stress S Figure 23.

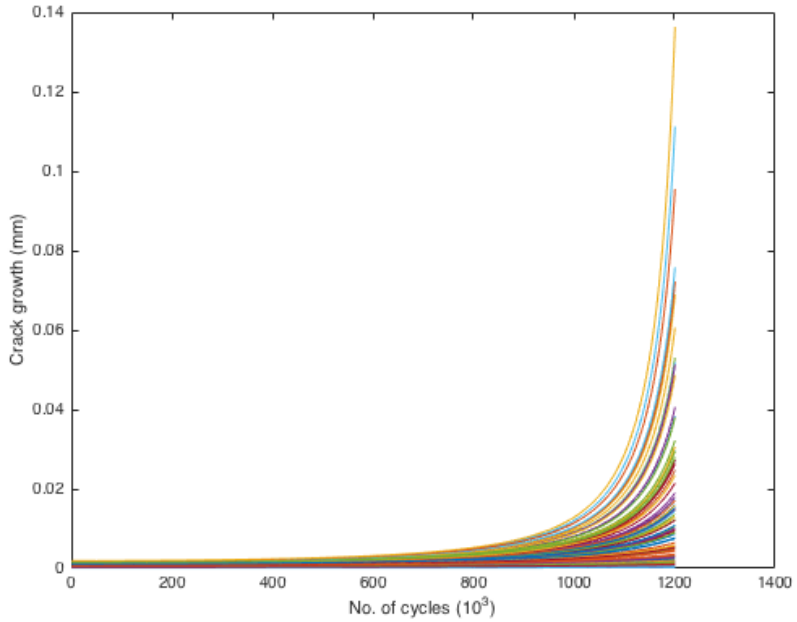

Figure 23 Plot of Paris model for initial crack size uniformly distributed between (0.1-2mm).

- Plot of Paris model for growth of fatigue cracks with variable stress but with constant material parameters (C&m) and constant initial crack size Figure 24.

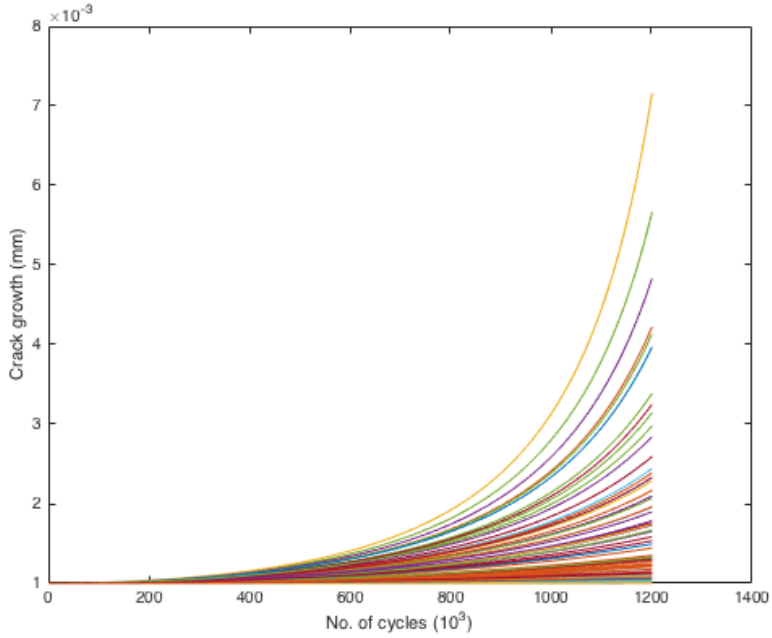

Figure 24 Plot of Paris model for stress uniformly distributed between (10-100 MPa)

- Plot of Paris model with variable F parameter but with constant material parameters (C and m) and constant initial crack size and also stress S Figure 25.

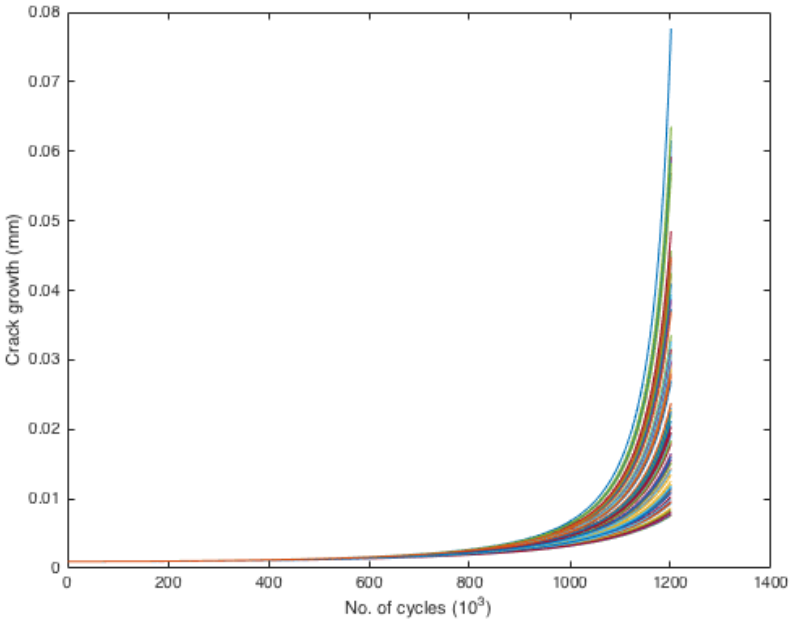

Figure 25 Plot of Paris model with variable F parameter but with constant material parameters.

- Plot of Paris model for growth of fatigue cracks with variable stress plotted as triangular distributed with parameters (a=0, b=0, c=100) but with constant material parameters (C & m) and constant initial crack size Figure 26.

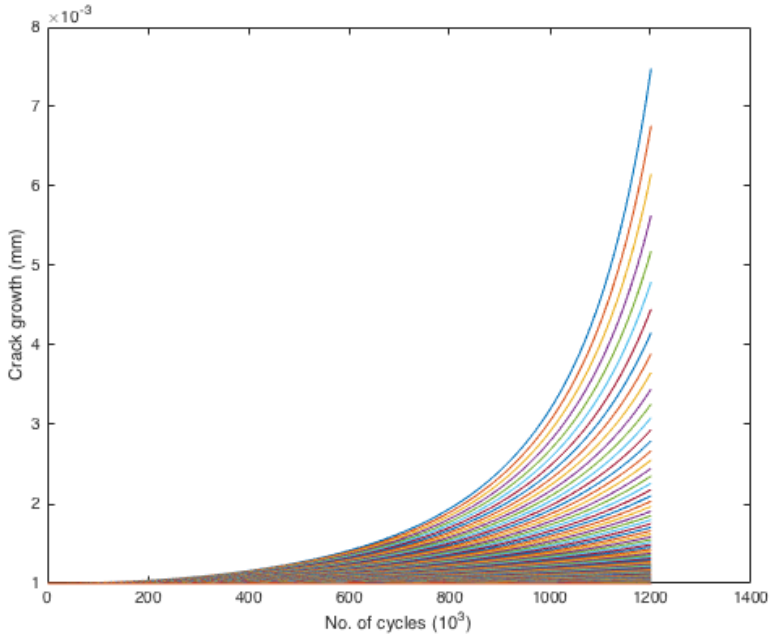

Figure 26 Plot of Paris model for growth of fatigue cracks with variable stress plotted as triangular distributed

- Plot of Paris model for growth of fatigue cracks with stress variation cycle by cycle but with constant material parameters (C & m) and constant initial crack size Figure 27.

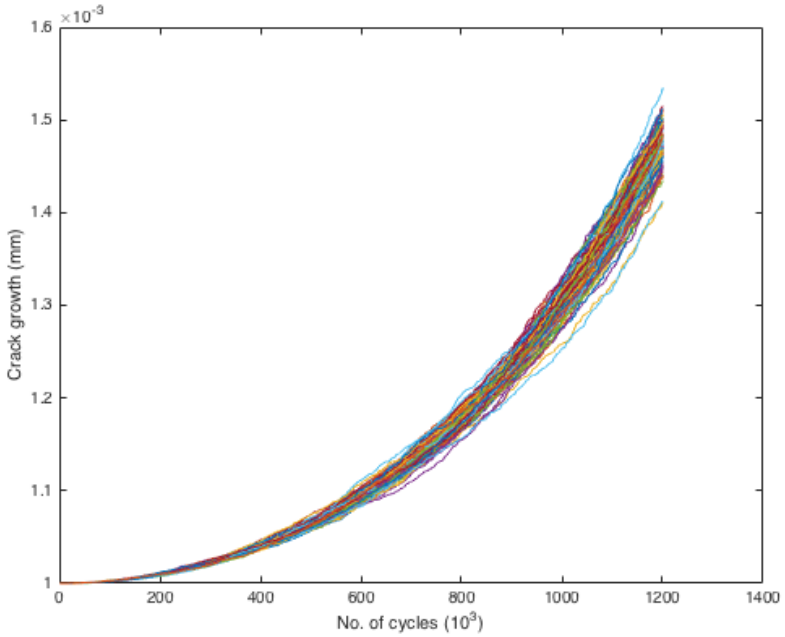

Figure 27 Plot of Paris model for growth of fatigue cracks with stress variation cycle by cycle

6.2 Simulation of Crack Growth and Inspections

For the calculation of pre-warning time and probability of detection of cracks, Monte Carlo simulations have been used. The inspections have also been introduced for the detection of cracks, when they are already initiated. For this purpose, a MATLAB (Mathworks, 2016) script was created to carry out the simulations (Appendix 1) and results are presented in the Figure 28.

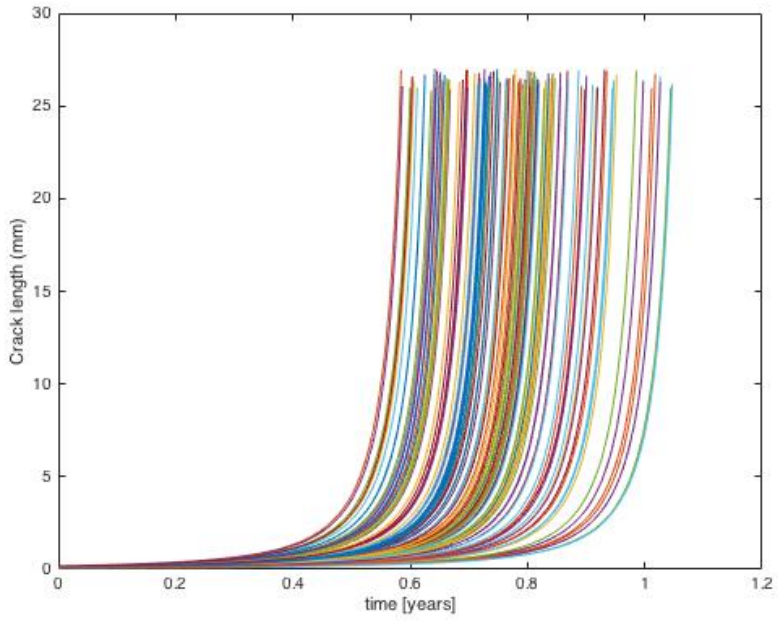

Figure 28 Simulation of 100 degradation paths

The crack growth is too fast only few months until failure (Figure 29). The reason for this is that sampled random stress ranges are from a triangular distribution, and not from the distribution we can establish based on the realistic data. Using a triangular distribution will result in too many cycles with high stress range. Thus, the crack grows faster than in the simulations based on realistic data.

Inspections are also introduced in the code, with constant inspection intervals tau. They are simulated then if the crack is above a limit. If so, it will be repaired. If the crack grows fast, it can be that it is not detected, thus the probability of detection is not 100 %, but below (in the example below *P*_detection = 1). *P*_repair = 1, because we assumed that all cracks detected are actually also repaired.

Based on the simulations, statistics of the failure time (time to failure) and the pre-warning time (the time between detection and failure, given that the crack actually is detected) has been made and presented in Figure 29 and Figure 30 respectively. *P*_det and prewarning time are two parameters that are input in NOWIcob.

Table 4 Failure time in years

Failure time (years)		
Mean failure time	Maximum failure time	Minimum failure time
0.7918	1.1315	0.5806

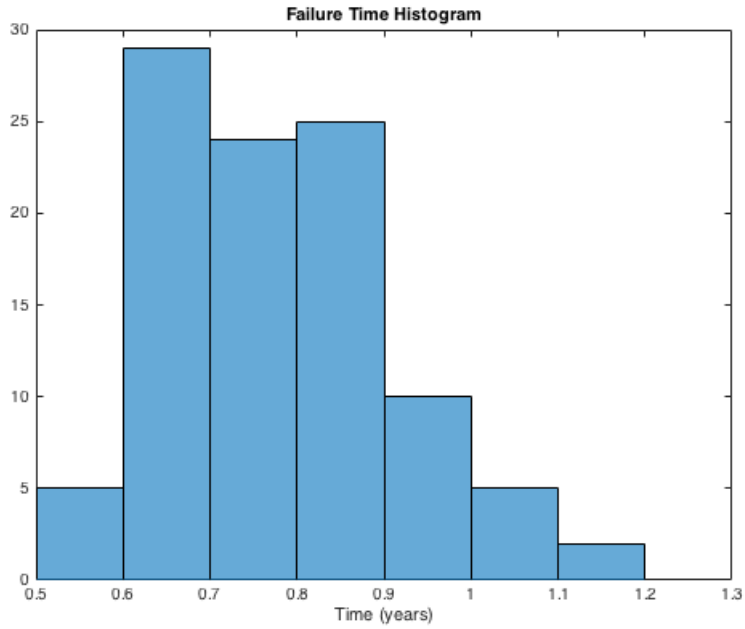

Figure 29 Failure Time Variation represented by histogram

Probability of detection:

P_detection = 1

Probability of repair given detection:

P_repair = 1

Table 5 Prewarning time in years

Prewarning time (years)		
Mean prewarning time	Maximum prewarning time	Minimum prewarning time
0.1014	0.1400	0.0586

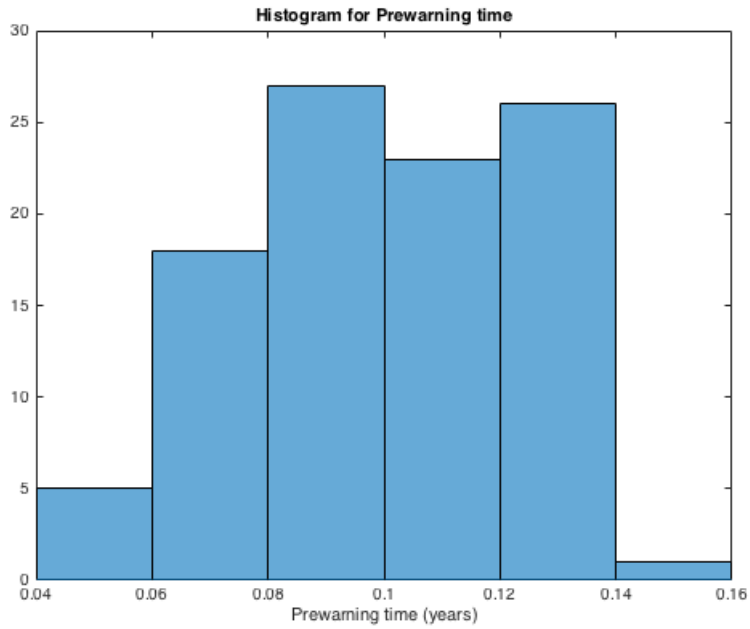

Figure 30 Histogram for Prewarning time

6.3 Results of Degradation Modelling Using Gamma Process

The results of degradation modelling by gamma process are presented in this chapter. The results discussed in this section supports the understanding of the degradation modelling explained in chapter 3.

Assumptions and Limitations

The data set used in the analysis is based on the one presented by Ceciliano J. (2010) for deterioration modelling of coatings in hydropower turbines.

6.3.1 Gamma Data Analysis

Parameter estimation

The estimates for the gamma process parameters α, β *and* η are presented in the table below.

Parameters	**Estimates**
$\boldsymbol{\alpha}$	2.642
$\boldsymbol{\beta}$	1.266
$\boldsymbol{\eta}$	0.109

6.3.2 Simulations

Monte Carlo Simulations can be used to generate random deterioration paths. For this purpose, a MATLAB (Mathworks, 2016) script was created to carry out the simulations (Appendix 2). The resulting hundred simulation paths for degradation are shown in Figure 31. X(t) is a random variable describing the deterioration or crack growth at time '*t*' and is measured on a continuous scale. For extension of the applications of maintenance optimization models, it is further beneficial to find the mean time for the degradation process to reach specific conditions. For example, the limits X_P and X_F are important in our analysis which corresponds to pre-warning time $T_{det.}$ When the degradation approaches the X_P, it is large enough to be detected by inspections. On the other hand, if the limit of X_F is crossed, the item is considered to be in the failed state and will be replaced correctively (corrective replacement). At time $t = 0$, there are no cracks in the system (minor inherent cracks from manufacturing are neglected) and the degree of degradation /condition is $X(t) = 0$, while the threshold has been defined as the degree of degradation/condition $X(t) = 5$.

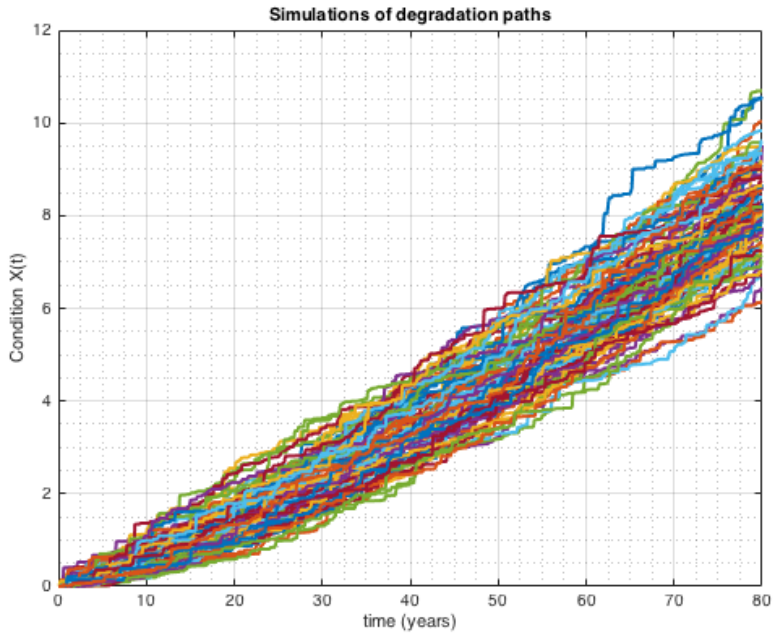

Figure 31 Simulation of 100 degradation paths using Monte Carlo.

6.3.3 Calculation of Different Levels of Degradation

Using the Matlab script given in the Appendix 2, 100 random degradation paths has been simulated. Also the mean time to reach the given condition X(t) has been calculated by

running a large number of simulations. For each generated random degradation path, there is a random unique time for the process to cross a specific threshold/level. The level X_P corresponds to the potential failure P and is the first time where we can observe the degradation/potential failure. This level corresponds to the value of condition $X(t) = 2$ in Figure 31. The mean time to reach this condition from all degradation paths has been calculated along with standard deviation. Likewise, the level 4 relates to the condition in which the system is considered to be in the failed state X_F and the value for this state is taken $X(t) = 5$. Also the mean time to reach this system failure condition is calculated from simulations and results are presented in the table below.

Table 6 Mean time and standard deviation for critical levels in degradation calculated from Monte Carlo Simulations

Condition *X(t) Degradation*	Min. Time (Years)	Max. Time (Years)	Mean Time (Years)	Standard Deviation (Years)
Level 1 (X_P)	13.4000	34.9000	26.4930	4.5942
Level 4 (X_F)	40.8000	64.6000	53.7670	4.7401

6.3.4 Calculation of the PF-interval:

Once the initial calculations have been made for the two critical degradation conditions, the next step was the determination of PF interval. This interval is actually the difference of the failure time to the initial detection time. This time actually represent the time interval since the crack has been detected until it reaches a critical level and is called the average pre-warning time. It denotes the time window to carry out preventive maintenance tasks to survive from the failure of the system at later stage. A boxplot of the PF interval is presented in Figure 32.

Min. Time PF (Years)	Max. Time PF (Years)	Mean Time PF (Years)	Standard Deviation PF (Years)
13.6000	38.7000	27.3770	5.1683

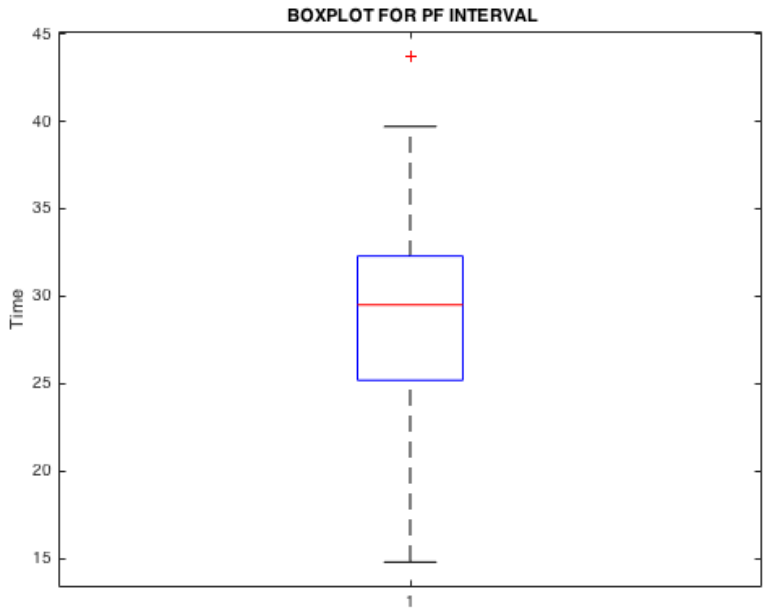

Figure 32 Boxplot for average pre-warning time

Chapter 7

Conclusions and Recommendations

This thesis project aimed to propose suitable models to capture the degradation of components of offshore wind turbines over time. Simple/loose integration of degradation, inspection and maintenance for the NOWIcob decision support tool has been investigated, by developing translators from detailed degradation models. Numerical methods and simulations (e.g., Monte Carlo Simulations) has been employed for this purpose. The linear elastic fracture mechanics model based on Paris law, and the Gamma process have been studied in this project. Monte Carlo simulations have been used for both of the models. According to the findings from the Paris law, following conclusions can be drawn:

- Shape and geometry of cracks contribute to their development.
- The material parameters C and m has no significant effect on the crack growth, although these are important characteristics of the material.
- For the development of fatigue crack growths, the most important factor are the variable stresses which are resulted from different kinds of loads i.e., wave load, wind load or current loads.
- The growth of cracks is too fast for the developed crack growth model, only few months until failure because this analysis is based on the stresses from triangular distribution, which resulted into too many cycles with high stress range. Hence the crack growth is faster due to this reason.
- Provided the values used for the parameters in the model, i.e., for tau, detection limit and acceptance limit, the probability of detection of cracks has been found to be one and also the probability of repair is one, it means that every crack which has been detected, will also be repaired before failure. Changing the values of these parameters would change the results accordingly.

The gamma process has been extensively applied in the previous studies on deterioration modelling. It can capture the variability because of its explicit dependence over time. Monte Carlo approach has been used to find the mean time to approach the degradation level to

reach the detection stage and also to the failure stage. Based on the results obtained from the gamma process, the following conclusions can be drawn:

- Gamma process is a flexible model because it uses three parameters, i.e., α, β and η which makes possible to model a realistic degradation process.
- The gamma process is capable to take the process variance in both the directions, i.e., the variability in the x-axis (condition) and the y-axis (time).
- The results from gamma process show that the failure time is expanded on decades and so likewise the PF-interval.

In general, by comparing the results from both models, it can easily be concluded that each model has unique parameters, so have unique results. The loose integration used in this work is an applicable approach to be employed in the NOWIcob to capture the degradation and inspection in the model.

Recommendations for Future Research

With the knowledge gained through this project, some recommendations for future research can be formulated.

- PoD curves can be employed in the code for detailed analysis.
- Improvement can be made in the models presented in the thesis for further studies.
- New models can be used to compare the results
- Risk-Based Inspection methodology for offshore wind turbine structures can be employed to minimize the inspection and repair costs.

References

Abdel-Hameed M. A gamma wear process. *IEEE Trans Reliab 1975;24(2):152–3.*

Barlow RE, Proschan F. *Mathematical theory of reliability. New York: Wiley; 1965*.

Beier, H.T. , B. Schork, J. Bernhard , D. Tchoffo Ngoula , T. Melz, M. Oechsner and M. Vormwald, Simulation of fatigue crack growth in welded joints, Material science and engineering technology, Vol 46 Issue 2, p. 110-122, February 2015.

Ceciliano, J. N. 2010. Modelling deterioration of coatings in hydropower turbines. Norwegian University of Science and Technology, Trondheim, Norway. Master's Thesis.

Dowling, N.E. (1993), Mechanical Behaviour of Materials, *Englewood Clifs, NJ: Prentice Hall.*

Hofmann, M., Sperstad, I.B, Kolstad, M. (2015), *Technical documentation of the NOWIcob tool (DB. 1-2), report no. TRA7374, SINTEF Energy Research, Trondheim*.

Kallehave D, Byrne BW, LeBlanc Thilsted C, & Mikkelsen KK. 2015. Optimization of monopiles for offshore wind turbines. *Phil. Trans. R. Soc. A, 373,* 20140100. http://dx.doi.org/10.1098/rsta.2014.0100.

LEANWIND Consortium (2015). *Optimised maintenance and logistic strategy models (D.4.2).*

Malhotra Sanjeev, (2009), "Design Considerations for Offshore Wind Turbine Foundations in the United States," International Society of Offshore Polar Engineers, Osaka, Japan, June 24-26, 2009.

Meeker, W. Q. and Escobar, L.A. (1998), *Statistical Methods for Reliability Data, Wiley, New York*.

Pandey MD, Yuan X-X, van Noortwijk JM. A comparison of probabilistic deterioration models for life-cycle management of structures. *Struct Infrastruct Eng 2007.*

References

Rausand, M. and Høyland, A. (2004), *System Reliability Theory – Models, Statistical Methods, and Applications, 2nd edition, Wiley, Hoboken.*

Ritche, R.O. , Mechanisms of fatigue-crack propagation in ductile and brittle solids, International Journal of Fracture 100: 55-83, 1999

Sanjeev Malhotra (2011). Selection, Design and Construction of Offshore Wind Turbine Foundations, Wind Turbines, Dr. Ibrahim Al-Bahadly (Ed.), ISBN: 978-953-307-221-0, InTech, Available from: http://www.intechopen.com/books/wind-turbines/selection-design-and-construction-of-offshore-wind-turbine- foundations

Singpurwalla ND. Survival in dynamic environments. *Stat Sci 1995; 10(1):86–103.*

Singpurwalla ND, Wilson SP. Failure models indexed by two scales. *Adv Appl Probab 1998;30(4):1058–72.*

van Noortwijk, J.M. (2009), "A survey of the application of gamma processes in maintenance", *Reliability Engineering and System Safety, vol. 94, no. 1, pp. 2-21.*

Ziegler L, Voormeeren S, Schafhirt S, & Muskulus M. 2016. Design clustering of offshore wind turbines using probabilistic fatigue load estimation. *Renewable Energy*. DOI: 10.1016/j.renene.2016.01.033.

SINTEF Energy Research, 2016, available online: https://www.sintef.no/projectweb/leanwind/ (last accessed 2016-01-15).

International Energy Agency, 2016, available online: http://www.iea.org/topics/renewables/subtopics/wind/ (last accessed 2016-05-21)

DNVGL, 2015. Probabilistic methods for planning of inspection for fatigue cracks in offshore structures. Recommended practice DNVGL-RP-0001.

DNVGL, 2016, available online: http://rules.dnvgl.com/docs/pdf/dnvgl/ST/2016-04/DNVGL-ST-0126.pdf (last accessed 2016-05-21)

References

Siemens Wind Power, available online: http://www.energy.siemens.com/nl/en/renewable-energy/wind-power/platforms/g4-platform/wind-turbine-swt-3-6-120.htm#content=Design (last accessed 2016-05-22)

http://www.electropedia.org/iev/iev.nsf/display?openform&ievref=192-06-07 (last accessed 2016-06-29)

Appendix 1

Matlab script to run fatigue crack growth, a linear elastic fracture mechanics model with inspections. The same script can be used to plot statistics of failure time, average pre-warning time and probability of detection.

```
clc
close all
clear all

rng('shuffle') %initialize random number generator

% Material properties
C = 1*10^(-11);  %(m/cycle)/(Mpa sqrt(m))^m*
F=1;
m_star = 3;
e = 1-(m_star/2);

%Number of Monte Carlo iterations (Number of simulations'n'):
j_max = 100;
%Number of repetitions before plotting:
f_plot = 1000;

%random initial crack size (triangular)
a0_min = 0.05* 10^(-3);
a0_middle = 0.1 * 10^(-3);
a0_max = 0.2 * 10^(-3);
pd2 = makedist('Triangular','a',a0_min,'b',a0_middle,'c',a0_max);
a_0 = random(pd2,j_max,1);
%Critical crack size
a_max = 27 * 10^(-3);

%random stress cycles (triangular)
pd = makedist('Triangular','a',0,'b',0,'c',100);
S = 1000000; %number of precalculated stress ranges
d_S = random(pd,S,1); %random stress range in MPa
%number of cycles having the same stress range
n_rep = 50;
%max(d_S)
%min(d_S)

%time equivalent to one stress cycle:
delta_t = 0.755309352; %at tower bottom (TB)

%inspection interval
tau = 30/30; %[months]
tau = tau*(30*24*60*60); %Convert from months to seconds

%detection limit
a_detect = 2 * 10^(-3); %mm
%acceptance limit
a_accept = 2 * 10^(-3); %mm (if a_accept = a_detect --> all cracks that are detected are repaired
immediately)

%Create matrix with zeros
```

```
a_1 = zeros(10000,j_max); %crack length in mm is stored in this matrix
t_failure = zeros(1,j_max); %failure times (time when crack cross failure limit)
det = zeros(1,j_max); %will be set to 1 if crack is detected before failure
rep = zeros(1,j_max); %will be set to 1 if crack is repaired before failure
t_det = zeros(1,j_max); %detection time, if crack is detected
t_prewarning = zeros(1,j_max); %prewarning time, if crack is detected

s = 1;

for j=1:j_max %j_max Monte Carlo iterations
j
n = 1; %cycle counter, n=0 is the initial crack length at t=0
n2 = 1; %counter when data is stored for plotting
n_plot = 1 + f_plot * n_rep;
a_n = a_0(j); %crack length at t = 0
a_1(n,j) = a_0(j);
X1(1) = 0;
z = 0;
detection = 0;
t_insp = tau; %time of first inspection
while a_n<a_max %Random crack growth from initial crack size_0(j) until crack is larger than critical
crack size a_max
delta_S = d_S(s); %Random stress in MPa
s = s + 1; %increase s by 1 to select next delta_S in the next step
if s>S %i.e. if all random stress ranges are used
d_S = random(pd,S,1); %simulated additional S random stress ranges
s = 1; %reset s to start using random stress von beginning of stress range vector
end
%delta_a = C * (F * delta_S * sqrt(pi*a_n)).^m_star;
%a_n = a_n + delta_a;
a_n = (a_n^e+n_rep * e * C * (F * delta_S * sqrt(pi)).^m_star )^(1/e);
n=n+n_rep;

%Check if inspections and repair
if (((n-1)*delta_t)>= t_insp) %inspection
if a_n >= a_detect
if det(1,j) == 0; %first time we detect this crack
det(1,j) = 1;
t_det(1,j) = n*delta_t; %store detection time
end
if a_n >= a_accept %repair
rep(1,j) = 1;
end
end
t_insp = t_insp + tau;
end %end inspection

if (n == n_plot) %store results for plotting if t_plot is reached or passed
n2 = n2 + 1;
if n2 > size(a_1,1) %increase matrix size if required
a_1 = [a_1; zeros(10000,j_max)];
end
a_1(n2,j) = a_n;
n_plot = n_plot + f_plot * n_rep;
end
end %End crack growth
t_failure(1,j)=(n-1)*delta_t;
if det(1,j) == 1 %calculate prewarning time if crack is detected
t_prewarning(1,j) = t_failure(1,j) - t_det(1,j);
end
```

```
end %end Monte Carlo iterations

a_1 = a_1 * 1000; %convert crack length from m to mm
%Remove all zero values and replace by NaN (not a number):
a_1(find(~a_1))=NaN;

%Create vector with cycles where data is plotted
n_max = size(a_1,1);
X1 = zeros(n_max,1);
X1(1) = 0;
for i = 2:n_max
X1(i) = X1(i-1) + f_plot * n_rep;
end
%Create time axis vector:
T1 = X1 * (delta_t/(60*60*24*365)); %time in years

figure,plot(T1,a_1)

%xlabel('No. of cycles')
xlabel('time [years]')
ylabel('Crack length (mm)')

%Statistics:
t_failure = t_failure/(60*60*24*365); %convert to years
disp('Failure time [years]')
disp('====================')
disp('Mean failure time:')
mean(t_failure)
disp('Maximum failure time:')
max(t_failure)
disp('Minimum failure time:')
min(t_failure)
%hist ogram(t_failure);

%Probability of detection:
disp('Probability of detection')
disp('=========================')
P_detection = sum(det)/j_max

%Probability of repair given detection:
disp('Probability of repair given detection')
disp('====================================')
P_repair = sum(rep)/sum(det)

%Prewarning time
t_prewarning(t_prewarning==0) = []; %remove zero elements in t_prewarning
t_prewarning = t_prewarning/(60*60*24*365); %convert to years
disp('Prewarning time [years]')
disp('=======================')
disp('Mean prewarning time:')
mean(t_prewarning)
disp('Maximum prewarning time:')
max(t_prewarning)
disp('Minimum prewarning time:')
min(t_prewarning)
hist ogram(t_prewarning);
```

Appendix 2

Matlab script to perform degradation paths for gamma process and results for mean time to detect failure, failure level and PF interval.

```
%function simulation
%Write number of simulations 'n'
n=100;
plotting=3; %(1: pdf plot, 2:CDF plot, 3: Simulations paths)
%Parameters
a=2.642 %a=2.642;
b=1.266 %b=1.266;
eta=0.1091;
%Time interval
T=[0:0.1:80];
T=T';
[m]=size(T);
m=m(1)
alpha= zeros(m);
X=zeros(m,n);
for k=1:n
% Calculate shape parameter
for i=1:m
if i==1
alpha(i)=((T(i)/a)^b);
else
alpha(i)=((T(i)/a)^b-(T(i-1)/a)^b);
end
end
%generate ramdom values of delta X
DeltaX=zeros(m);
for i=1:m
DeltaX(i)=gamrnd(alpha(i),eta);
end
%Find commulative condition X(t), i.e. generate the n degradation pathes
for i=1:m
if i==1
X(i,k)= DeltaX(1);
else
X(i,k)=DeltaX(i)+X(i-1,k);
end
end
%Find expected value to reach a specific condition level
for i=1:m
if i==1
p(i)= DeltaX(1);
else
p(i)=DeltaX(i)+p(i-1);
end
end
%%%%%Specify which condition levels%%%%%%%
%level 1 --> time1. This is the level for potential failure P
% (that is the first time where we can observe the potential failure /
% degradation
%level 1 --> time1;
level1 = 2;
[r1,c1,v1]=find(p<=level1);
%level 2 --> time2;
```

```
level2 = 3;
[r2,c2,v2]=find(p<=level2);
% level3 --> time3;
level3 = 4;
[r3,c3,v3]=find(p<=level3);
% level4 --> time4.  This is the failure level F.
level4 = 5;
[r4,c4,v4]=find(p<=level4);
time1(k)=T(length(v1));
time2(k)=T(length(v2));
time3(k)=T(length(v3));
time4(k)=T(length(v4));
end
% PF-interval:
timePF = time4-time1;

%Results for level1:
time1;
mean_time1 = mean(time1);
mean_time1
std_time1 = std(time1);
std_time1
min_time1= min(time1);
min_time1
max_time1 = max(time1);
max_time1
% Histogram
hist(time1)

% ..
mean(time2);
std(time2);
% ..
mean(time3);
std(time3);
%Results for level4:
level4
time4;
mean_time4 = mean(time4);
mean_time4
std_time4 = std(time4);
std_time4
min_time4 = min(time4);
min_time4
max_time4 = max(time4);
max_time4
failureRate = 1./mean_time4;
failureRate
% Histogram
hist(time4)
%Normal distribution fit for time4
[normMean, normSD, normMeanCI, normSDCI]=normfit(time4);
normMean
normSD
normMeanCI
normSDCI
%exponential distribution fit for time4
[expMean, expMeanCI]=expfit(time4);
expMean
expMeanCI
```

```
%Results for PF-interval
meanPF = mean(timePF);
meanPF
minPF = min(timePF);
minPF
maxPF = max(timePF);
maxPF
stdPF = std(timePF);
stdPF
boxplotPF = boxplot(timePF)
boxplotPF
xlabel('')
ylabel('Time')
title('BOXPLOT FOR PF INTERVAL')
% sortPF = sort(timePF);
% sortPF
%Histogram
hist(timePF)
%plot(T,X);
% compute commulatives probabilities
f=(0:1/n:1);
t1=[0;sort(time1')];
t2=[0;sort(time2')];
t3=[0;sort(time3')];
t4=[0;sort(time4')];
%%%%%PLOTS%%%%%%%%
if plotting==1
%%%%%%%%%%%%Probaility density functions%%%%%%%%%%%%%%%%%%%%%%%%
[f1,t1i] = ksdensity(t1);
[f2,t2i] = ksdensity(t2);
[f3,t3i] = ksdensity(t3);
[f4,t4i] = ksdensity(t4);
hand=plot(t1i,f1,'g',t2i,f2,'y',t3i,f3,'m',t4i,f4,'r');
set(hand, 'LineWidth', 4);
grid on
grid(gca,'minor')
title('Probability Density Function (PDF)')
xlabel('time (years)')
ylabel('Probability Density')
end
%%%%%%Cummulative Distributions%%%%%%%%%%%%
if plotting==2
hand=plot(t1,f,'g',t2,f,'y',t3,f,'m',t4,f,'r');
set(hand, 'LineWidth', 2);
grid on
grid(gca,'minor')
title('Cummulative Distribution Function (CDF)')
xlabel('time (years)')
ylabel('Probability')
end
%%%%%%%%%Simulations%%%%%%%%%
if plotting==3
hand= plot(T,X);
set(hand, 'LineWidth', 2);
grid on
grid(gca,'minor')
title('Simulations of degradation paths')
xlabel('time (years)')
ylabel('Condition X(t)')
end
```

```
% end
```

Appendix 3

Matlab script to plot degradation paths based on Paris law.

```
function crack_growth
C = 1*10^(-11);   %(m/cycle)/(Mpa sqrt(m))^m*
m_star = 3;
a_0 = 1*10^(-3);    %in m


delta_S = 100;    %Mpa

F = [1,1.12];
N_F = length(F);



N = 0:1000:1200000;

M = length(N);




for N=1:M

a_1(N) = a_0 + C * ((F(1) * delta_S * sqrt(pi*a_0)).^m_star).*N;
a_0 = a_1(N);

end


figure,plot(a_1)
xlabel('No. of cycles (10^3)')
ylabel('Crack growth (mm)')

a_0 = 1*10^(-3);    %in m

for N=1:M
```

```
a_2(N) = a_0 + C * ((F(2) * delta_S * sqrt(pi*a_0)).^m_star).*N;
a_0 = a_2(N);

end


figure,plot(a_2)
xlabel('No. of cycles (10^3)')
ylabel('Crack growth (mm)')
```